Plan of the lectures

Monday
description, technical and practical advices to use RAMSES.
tests and problems

Tuesday
Numerical schemes, hydro and mhd solvers, stability

Wednesday
More about numerical schemes – The issue of div B
AMR issues and gravity

History of RAMSES

RAMSES has been written by Romain Teyssier (Teyssier 2002)

Originally designed for cosmology simulations
Amongst the largest cosmology simulations have been done with RAMSES

The first version handled dark matter particles (interaction only through gravity) and hydrodynamics

The particles are projected onto the mesh and the gravitational potential can be calculated using grid techniques (unlike what is generally done in SPH for example)

The adaptive mesh refinement (AMR) scheme allows to calculate accurately the gravitational potential in regions where there are important small scale variations

Cosmology with AMR

Particle-Mesh on AMR grids:
Cloud size equal to the local mesh spacing

Poisson solver on the AMR grid
Multigrid or Conjugate Gradient
Interpolation to get Dirichlet boundary
conditions (one way interface)

Quasi-Lagrangian mesh evolution:
roughly constant number of particles
per cell

$$n = \frac{\rho_{DM}}{m_{DM}} + \frac{\rho_{gas}}{m_{gas}} + \frac{\rho_*}{m_*}$$

Trigger new refinement when n > 10-
40 particles. The fractal dimension is
close to 1.5 at large scale (filaments)
and is less than 1 at small scales
(clumps).

Romain Teyssier
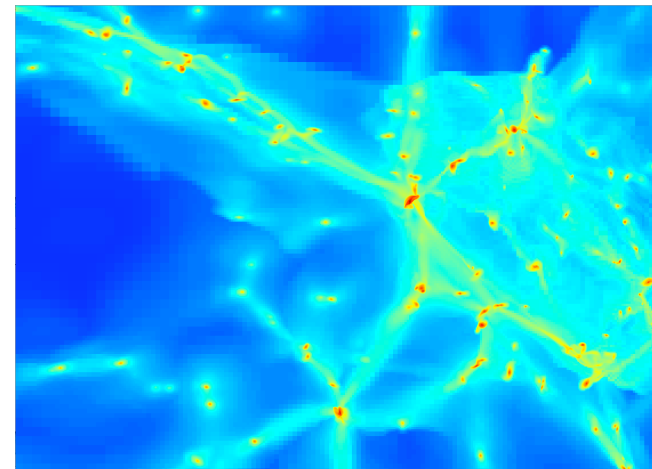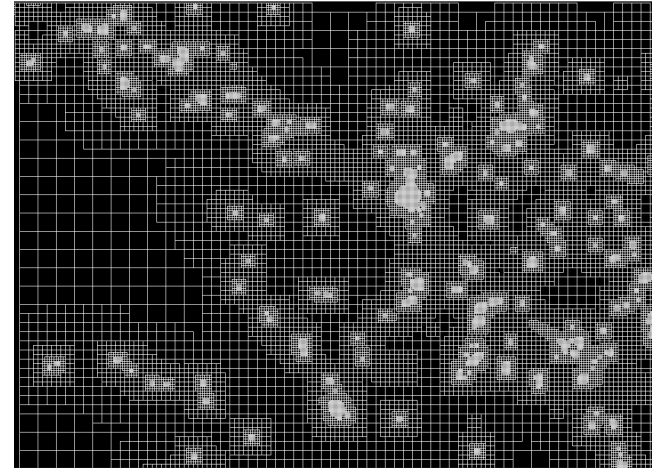
Further developments of RAMSES: magnetic field

The magnetic field has been introduced in the ideal MHD limit

Teyssier, Fromang, Dormy, 2006 : kinetic field (study dynamo)
Fromang, Hennebelle & Teyssier 2006 : ideal MHD

Use finite volume methods, 2nd order accuracy in time and space
Constraint transport schemes

Non ideal MHD effects have been introduced

Masson, Teyssier, Mulet-Marquis, Hennebelle and Chabrier 2012

Explicit treatment of the non-ideal mhd terms

Further developments of RAMSES: radiative transfer
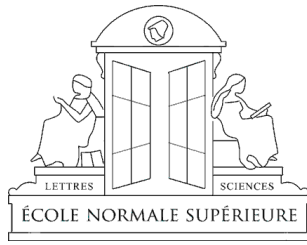
Explicit treatment

Aubert & Teyssier 2010

Rosdahl et al. 2010

Implicit treatment

Commerçon et al. 2011
grey transfer and diffusion approximation
Not publically available yet

Finite *volume* methods for compressible MHD

Patrick Hennebelle
Thanks to
Romain Teyssier and Sébastien Fromang

Summary of the lecture

1) Introduction
    -stability
    -MHD equations, standard and conservative forms
    -Godunov-type methods and Riemann problems

2) Riemann solver
    -exact hydrodynamical solver
    -ROE solver
    -HLL type solvers

3) High order schemes

4) 1D and 2D Numerical tests: comparing the solvers

5) MultiD MHD
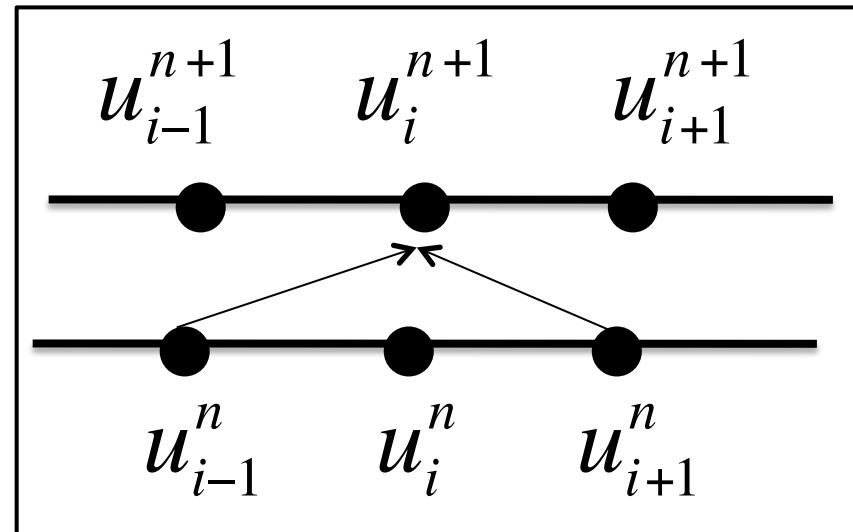   -Specificity of the MultiD MHD equations
    -the methods

6) 2D Numerical tests: comparing the methods

Introduction

Explicit methods and stability

We consider the simple advection equation:
a some constant.

$$\partial_t u + a \partial_x u = 0$$

Let us discretize it:

A possible and appealing choice is:

$$\Rightarrow \frac{u_i^{n+1} - u_i^n}{\Delta t} + a \frac{u_{i+1}^n - u_{i-1}^n}{2\Delta x} = 0$$

(subscript timestep, underscript position)

=>This method turns out to be unstable…

Physically this is because, information is "upwind". It should come only from the regions from which the flow is coming. Can be interpreted as a negative viscosity otherwise.

Mathematically, this can be shown using von Neumann analysis.
Let Fourier transform the mesh:

$$u_i^n = \sum A_k^n \exp(-ikx_i)$$

$$\Rightarrow A_k^{n+1} = A_k^n + \frac{a\Delta t}{2\Delta x}\left(-A_k^n \exp(-ik\Delta x) + A_k^n \exp(ik\Delta x)\right)$$

$$= A_k^n\left(1 + iC\sin(k\Delta x)\right), C = \frac{a\Delta t}{2\Delta x}$$

$$\Rightarrow \left|\frac{A_k^{n+1}}{A_k^n}\right|^2 = 1 + C^2\sin^2(k\Delta x) \geq 1$$

Thus, the modes are amplified at each time step leading to a strong instability.

Physically, the following discretization should get rid of this problem:
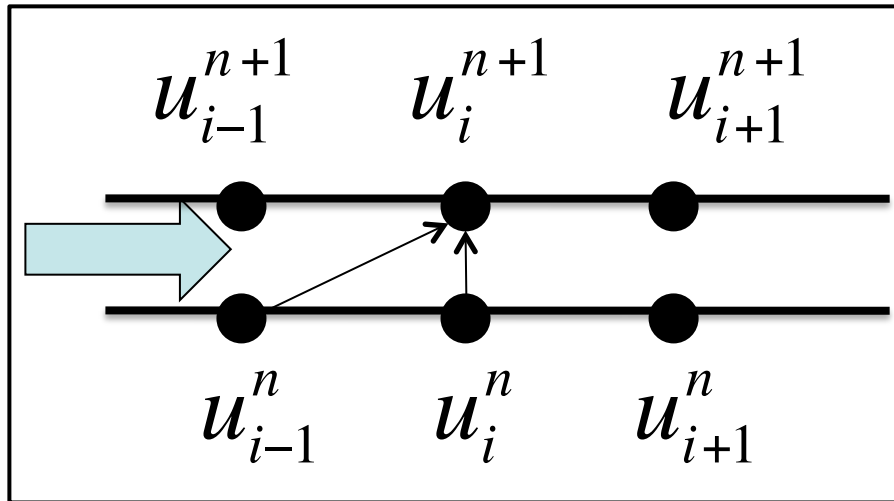
$$a > 0 \Rightarrow \frac{u_i^{n+1} - u_i^n}{\Delta t} + a \frac{u_i^n - u_{i-1}^n}{\Delta x} = 0$$

$$a < 0 \Rightarrow \frac{u_i^{n+1} - u_i^n}{\Delta t} + a \frac{u_{i+1}^n - u_i^n}{\Delta x} = 0$$

Let us check this mathematically:

$$u_i^n = \sum_k A_k^n \exp(-ikx_i)$$

$$\Rightarrow A_k^{n+1} = A_k^n + \frac{a\Delta t}{\Delta x}\left(-A_k^n + A_k^n \exp(ik\Delta x)\right)$$

$$= A_k^n\left(1 + C(-1 + \exp(ik\Delta x))\right), C = \frac{a\Delta t}{2\Delta x}$$

$$\Rightarrow \left|\frac{A_k^{n+1}}{A_k^n}\right|^2 = 1 - 2C(1 - C)(1 - \cos(k\Delta x))$$

Thus, the scheme is stable as long as C<1 which is called the:
Courant condition.

Physical meaning is clear: information should come from the nearest upwind neighbours.

In the case of more complex equations entailing various wave propagation, information comes generally from both the left and the right neighbours, depending on the *wave* which is considered.

Important messages:

-discretization matters a lot

-information should be upwind

-time step is a crucial issue

What is MHD ? Why MHD approximation ?

(Shu 1992, Kulsrud 2005 , ……)

In many astrophysical systems, the magnetic field is thought to play an important, sometimes dominant role (e.g. solar corona, solar wind, interstellar medium, accretion disk, jets…).

MHD equations are fluid equations and require that the collisional length must be small with respect to the size of the system considered. When this is not true Bolzmann equation should be used but considerably more difficult. In practice, MHD sometimes used even when this condition is not satisfied.

Even so, we should treat 2 fluids, electrons and ions: still very complex

But with four approximations, we can derive a single fluid set of equations leading to   ideal MHD equations:
   -local fluid neutrality (density of posivite charges = negative charges)
   -neglect the displacement current in Maxwell equations
   -neglect the electrons inertia
   -assume perfect conductor (no magnetic diffusivity, no Hall effect)

Non ideal, single fluid MHD may consider: resistivity, Hall terms, « ambipolar diffusion »

MHD equations, standard and conservative forms

$$\partial_t \rho + \vec{V}.\vec{\nabla}\rho + \rho\vec{\nabla}.\vec{V} = 0$$

$$\rho(\partial_t \vec{V} + \vec{V}.\vec{\nabla}\vec{V}) = -\vec{\nabla}P + (\vec{\nabla} \times \vec{B}) \times \vec{B}$$

$$= -\vec{\nabla}P - \vec{\nabla}\frac{\vec{B}^2}{2} + \vec{B}.\vec{\nabla}\vec{B}$$

$$\partial_t e + \vec{V}.\vec{\nabla}e + (\gamma-1)e\vec{\nabla}\vec{V} = 0$$

$$\partial_t \vec{B} + \vec{V}.\vec{\nabla}\vec{B} - \vec{B}.\vec{\nabla}\vec{V} + \vec{B}\vec{\nabla}.\vec{V} = 0$$

$$\vec{\nabla}.\vec{B} = 0$$

$$e = \frac{kT}{(\gamma-1)m_p}$$

$$\partial_t \rho + \vec{\nabla}.(\rho\vec{V}) = 0$$

$$\partial_t(\rho\vec{V}) + \vec{\nabla}(\rho\vec{V}\vec{V} - \vec{B}\vec{B} + P_{tot}I) = 0$$

$$\partial_t E + \vec{\nabla}.((E+P)\vec{V} - \vec{B}(\vec{B}.\vec{V})) = 0$$

$$\partial_t \vec{B} + \vec{\nabla} \times (\vec{B} \times \vec{V}) = 0$$

$$\vec{\nabla}.\vec{B} = 0$$

where

$$E = \rho e + \frac{1}{2}\rho\vec{V}^2 + \frac{1}{2}\vec{B}^2$$

$$P_{tot} = P + \frac{1}{2}\vec{B}^2$$

In 1D can also be written as:

$$\partial_t U + \partial_x F = \partial_t U + A\partial_x U = 0$$

$$U = (\rho, \rho u, \rho v, \rho w, B_y, B_z, E)$$

A is called the Jacobian

Its eigenvalues are the wave speeds.

$$F = \begin{cases} \rho u \\ \rho u^2 + P_T - B_x^2 \\ \rho uv - B_x B_y \\ \rho uw - B_x B_z \\ B_y u - B_x v \\ B_z u - B_x w \\ (E + P_T)u - B_x(uB_x + vB_y + wB_z) \end{cases}$$

$$B_x = cst$$

In 3D, we have:

$$\partial_t U + \partial_x F + \partial_y G + \partial_z H = 0$$

$$U = (\rho, \rho u, \rho v, \rho w, B_x, B_y, B_z, E)$$

$$\vec{\nabla}.\vec{B} = 0$$

Brief description of the MHD waves

The 1D MHD equations have seven eigenvalues or equivalently give rise to 7 waves.

2 Alfvén waves: transverse mode (analogous to the vibration of a string)

2 slow magneto-acoustic waves (coupling between Lorentz force and thermal pressure, B and ρ are anticorrelated)

2 fast magneto-acoustic waves (coupling between Lorentz force and thermal pressure, B and ρ are correlated)

1 entropy wave (contact discontinuity, does not propagate)

$$\lambda_{2,6} = u \pm c_a, \lambda_{1,7} = u \pm c_f, \lambda_{3,5} = u \pm c_s, \lambda_4 = u,$$
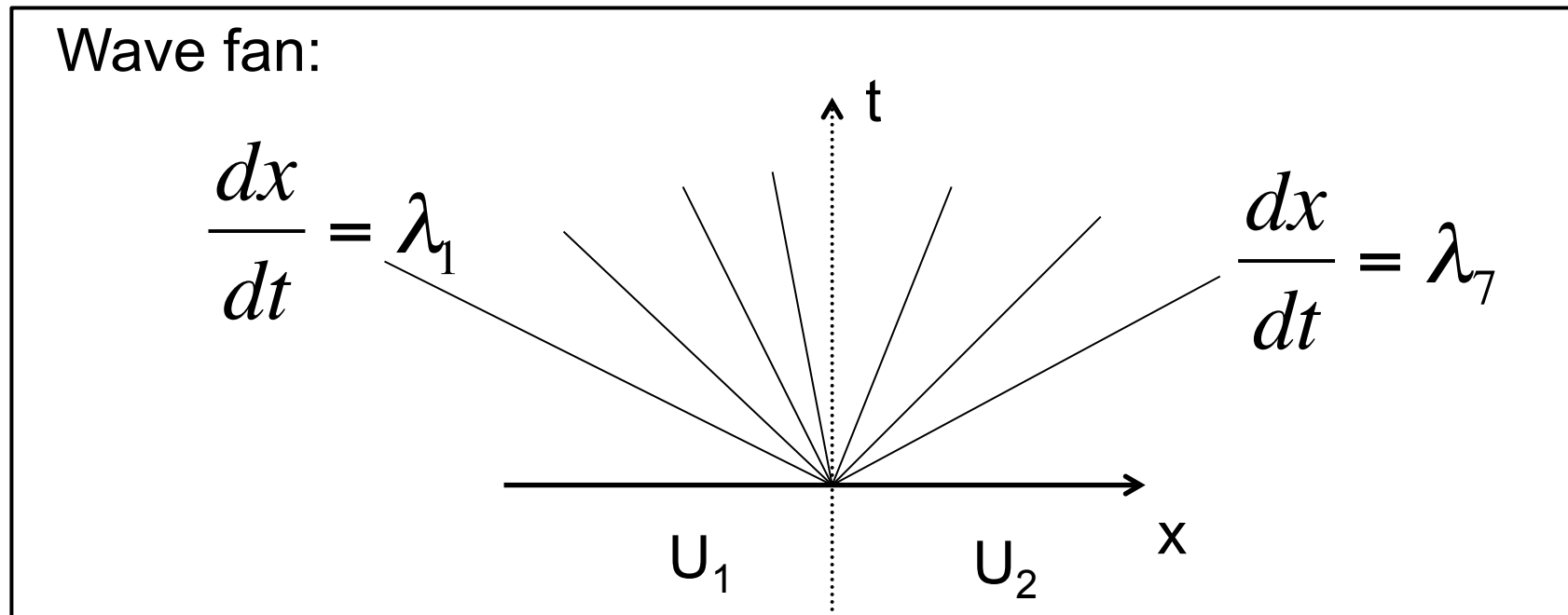
where

$$c_a = \frac{B_x}{\sqrt{\rho}}, c_{f,s} = \left(\frac{\gamma p + \vec{B}^2 \pm \sqrt{(\gamma p + \vec{B}^2)^2 - 4\gamma p B_x^2}}{2\rho} \right)^{1/2}$$

The wave velocities are such that:

$$\lambda_1 \leq \lambda_2 \leq \lambda_3 \leq \lambda_4 \leq \lambda_5 \leq \lambda_6 \leq \lambda_7$$

fast - Alfvén - slow - entropy - slow - Alfvén - fast

Therefore, some eigenvalues may coincide depending on the direction and the strength of the magnetic field (whereas hydro case is strickly hyperbolic).

Wave fan:

Godunov type methods

Originally developed to solve compressible hydrodynamical equations (Godunov 1959). Well suited to handdle shocks and discontinuities

=> This is why they are so commonly used in astrophysics. No need to introduce viscosity to stabilize the scheme. Discontinuities resolved in few cells.

Each computational cell represents a fluid volume with uniform density, velocity, energy inside the cell which represents the average values.
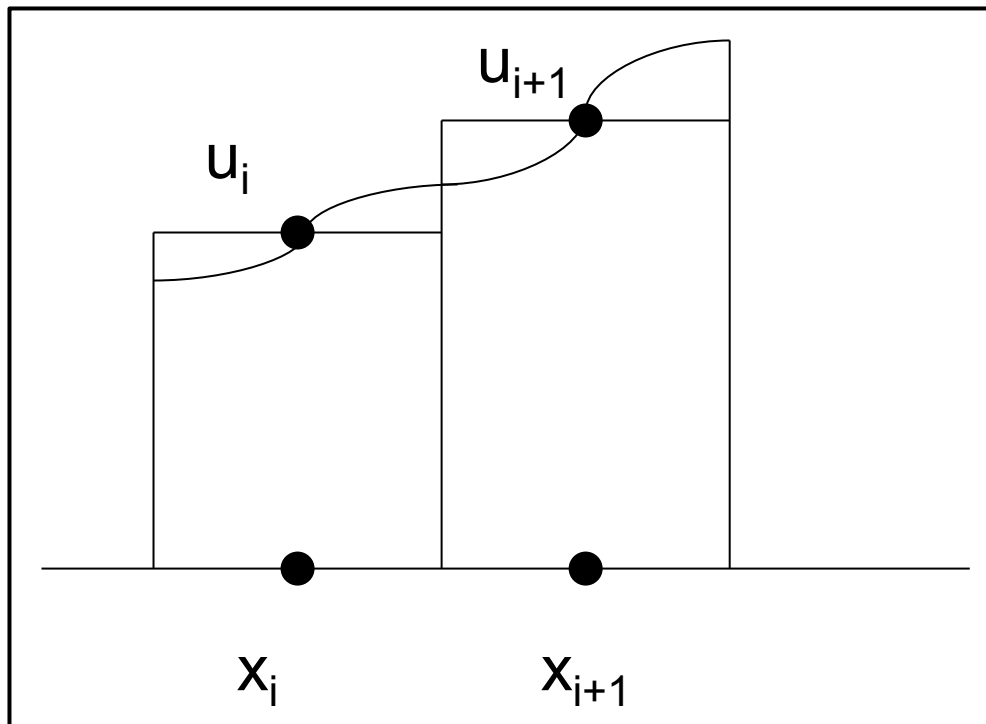
The total mass, momentum and energy within the cells are thus

$$dM_{cell} = \overline{\rho}_i dx(dydz), \, d\vec{P}_{cell} = \vec{\overline{P}}_i dx(dydz), \, dE_{cell} = \overline{E}_i dx(dydz),$$

$$with \; \overline{U}_i(t) = \frac{1}{\Delta x} \int_{x_{i-1/2}}^{x_{i+1/2}} U(t,x')dx' \quad (in \; 1D)$$

$$\overline{\overline{U}}_{i,j,k}(t) = \frac{1}{\Delta x \Delta y \Delta z} \int_{x_{i-1/2},y_{i-1/2},z_{i-1/2}}^{x_{i+1/2},y_{i+1/2},z_{i+1/2}} dx' dy' dz' U(t,x',y',z') \quad (in \; 3D)$$

The cells exchange flux of matter, momentum and energy between each others.
Philosophy different from finite difference methods, in which the discrete values represent the exact values of the quantity at the location, or from Fourier methods.
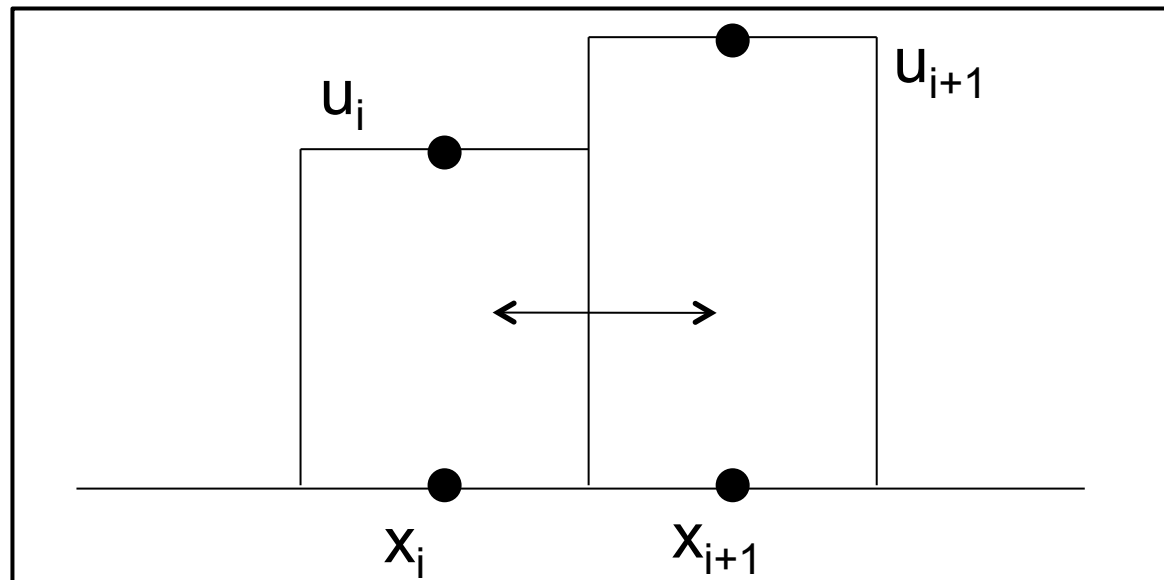
The *exact* discretized solution of $\partial_t U + \partial_x F = 0$ is given by:

$$\overline{U}_i(\Delta t) = \overline{U}_i(0) + \frac{\Delta t}{\Delta x}\left(\overline{F}(x_i) - \overline{F}(x_{i+1})\right)$$

$$where\ \overline{F}(x_i) = \frac{1}{\Delta t}\int_0^{\Delta t} dt\ F(U(t,x_i))\ (in\ 1D)$$

$$\overline{F}_{j,k}(x_i) = \frac{1}{\Delta t \Delta y \Delta z}\int_0^{\Delta t} dt \int_{y_j}^{y_{j+1}} dy \int_{z_k}^{z_{k+1}} dz\ F(U(t,x_i,y,z))\ (in\ 3D)$$

Note that:

-this is at this stage an exact solution, in practice however the fluxes are approximately calculated

-even if the fluxes are not correct, the method, *by construction*, conserves mass, momentum and energy exactly since the amount retrieve from one cell is exactly given to its neighbour

-this expression does not entail derivative but flux differences, this is why, discontinuities are well resolved. This is unlike finite difference methods or spectral methods.

The Riemann Problem

The question with the Godunov method is thus to estimate accurately the fluxes exchanged between two uniform states U_1 and U_2.
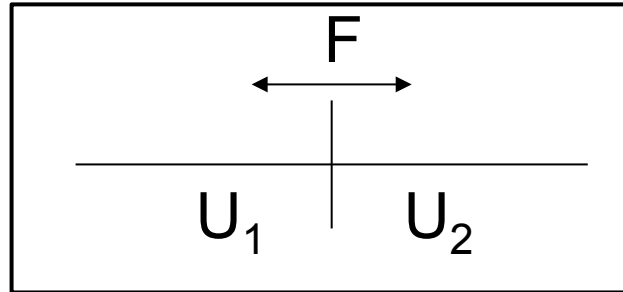
This is called the Riemann problem.

Since no characteristic scale is involved in the problem, it is *self-similar*. That is to say the pattern at (x,t) can be deduced from the pattern at (x',t'), U(x/t)=U(x'/t'). Thus, the flux exchanged between the 2 states is constant in time.

A central problem for Godunov type methods, is to have accurate « Riemann solvers » which resolve the Riemann problem at interface between cells and provide the flux.
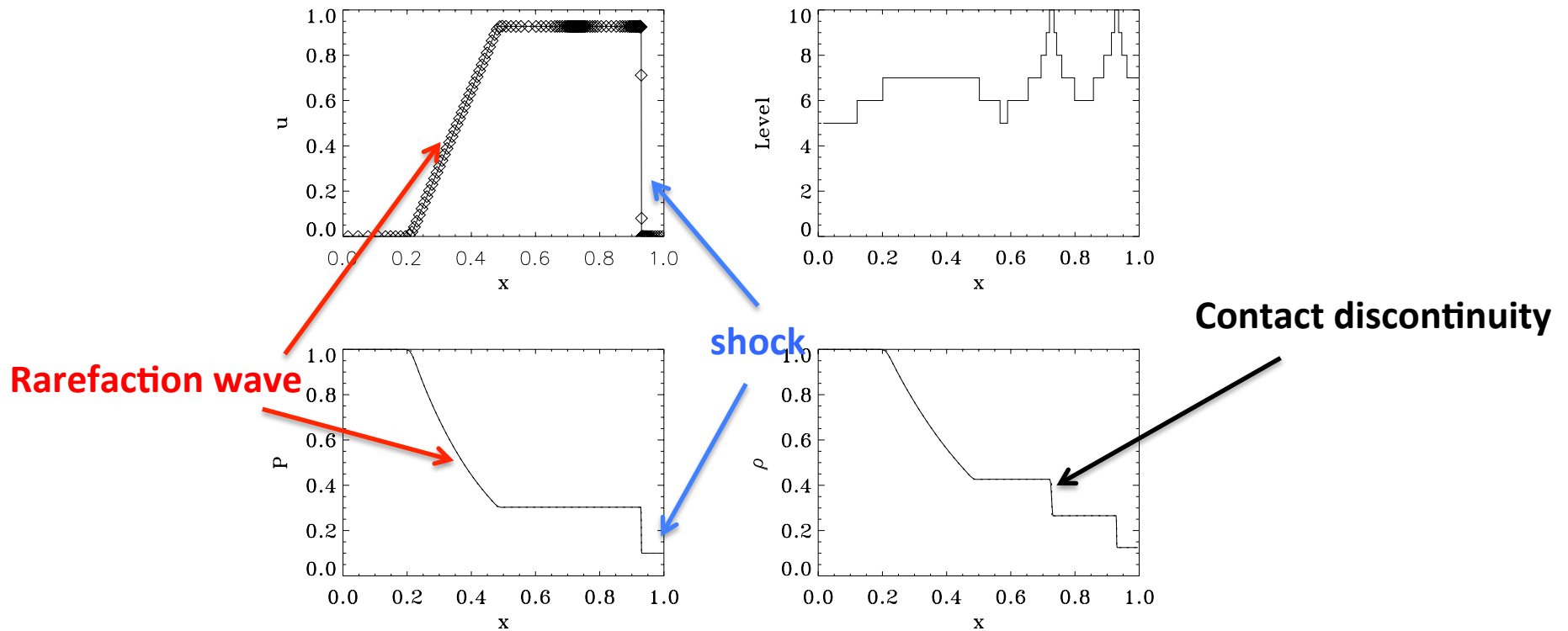
Solving the Riemann problem for non linear equations is in general a very difficult problem.

RIEMANN SOLVER

1D MHD

Exact hydrodynamical Riemann solver

-Hydrodynamical Riemann problem entails 3 non-linear waves, rarefaction wave, contact discontinuity and shock

-Exact hydrodynamical solver is known

-Need to perform several iterations

=>Accurate but expensive

=>Interest in having cheaper solvers

 In MHD, no exact solver is known (would be very expensive)

=> Need to find approximate solvers

Shock Jump conditions

Across a discontinuity (that is to say in any point), and in the frame moving with it, jump conditions apply: $F_1 = F_2$

In the laboratory frame, the discontinuity is moving at some speed λ_C. The jump relation can then be written as:

$$\lambda_c U_1 - F_1 = \lambda_c U_2 - F_2$$

To see this, let us consider again the equation: $\partial_t U + \partial_x F = 0$ and a control volume $[X_L, X_R]$. A corresponding integral form on the volume of control is:

$$F(U_R) - F(U_L) = \frac{d}{dt} \int_{X_L}^{x(t)} U(x,t)dt + \frac{d}{dt} \int_{x(t)}^{X_R} U(x,t)dt$$

$$= \frac{dx}{dt} U(x(t)_-,t) - \frac{dx}{dt} U(x(t)_+,t) + \int_{X_L}^{x(t)} \partial_t U(x,t)dt + \int_{x(t)}^{X_R} \partial_t U(x,t)dt$$

Thus, if $X_L \rightarrow X_R$, the integrals on the right hand side vanish and we obtain the relation.

# Solution of the Riemann Problem for linear hyperbolic systems

(Toro 1999)

Finding the solution of the Riemann problem is possible when the Jacobian A of the system is a constant matrix. As will be seen later, this turns out to be extremely useful.

Let us consider the simple linear advection equation: $\partial_t u + a \partial_x u = 0$
The solutions are simply given by: $f(x - at)$

Thus the rate of change of u along the characteristic curve dx/dt=a is zero. a is called the characteristic speed.
In this case the solution of the Riemann problem is very simple:
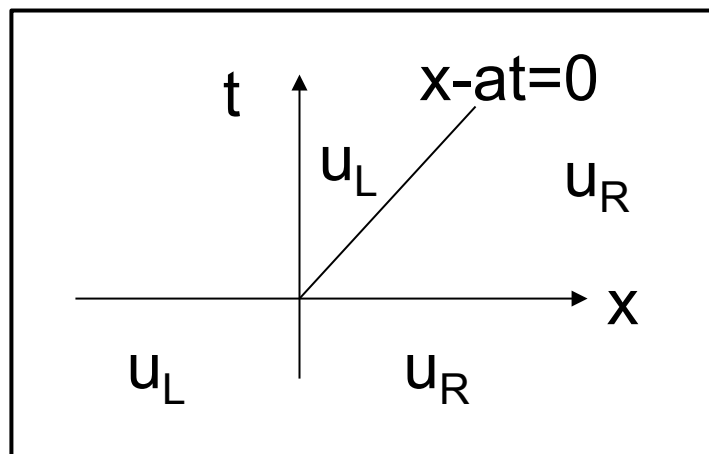
$$x - at < 0 \Rightarrow u = u_L$$

$$x - at > 0 \Rightarrow u = u_R$$

Now let us consider a linear system of m variables and equations.

$$\partial_t U + A\partial_x U = 0, A, \text{ a constant } m \times m \text{ matrix.}$$

Let us diagonalise A:

$$A = K^{-1}\Lambda K, \Lambda = \begin{bmatrix} \lambda_1 & . & . & . & 0 \\ 0 & . & & & . \\ . & & . & & . \\ . & & & \lambda_{n-1} & . \\ 0 & . & . & . & \lambda_n \end{bmatrix}, \quad K = [K^1,...,K^m], \quad AK^i = \lambda_i K^i$$

$$W = K^{-1}U \Rightarrow U = KW, \quad K^{-1}\partial_t U + K^{-1}A\partial_x U = \partial_t W + \Lambda \partial_x W = 0$$

Thus, the system is decoupled and the solution fo each W_i is just W_i (x-λ_it).
Coming back to U, we have:

$$U(x,t) = \sum_{i=1,m} W_i(x - \lambda_i t)K^i$$

Let us consider again the Riemann problem, U(x,0)=U_L for x<0 and U_R for x>0

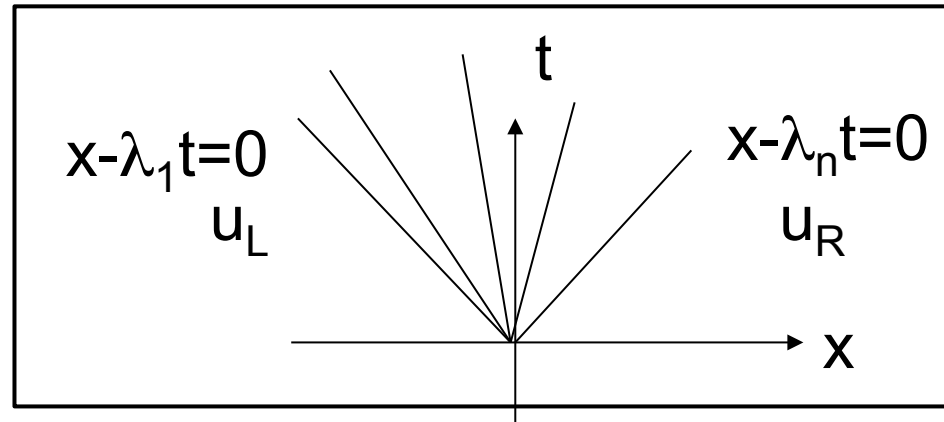We can write:

$$U_L = \sum_{i=1,m} \alpha_i K^i, \quad U_R = \sum_{i=1,m} \beta_i K^i$$

$$W_i = \alpha_i \text{ if } x < 0, \quad W_i = \beta_i \text{ if } x > 0.$$

For a given (x,t), there is an eigenvalue such that λ_I<x/t< λ_{I+1} :

$$U(x,t) = \sum_{i=I+1,m} \alpha_i K^i + \sum_{i=1,I} \beta_i K^i$$

Thus, we have the following picture:

The solution consists of m waves emanating from the origin.They constitute the wave fan. Each wave carries a jump discontinuity.

We can now estimate the flux exchanged between the cells that will be needed to advance the solution. The value of U at the interface is U(0):

$$U(0) = \sum_{i=I+1,m} \alpha_i K^i + \sum_{i=1,I} \beta_i K^i = \sum_{i=1,m} \alpha_i K^i + \sum_{i=1,I} (\beta_i - \alpha_i) K^i$$

$$= U_L + \sum_{i=1,I} (\beta_i - \alpha_i) K^i = U_R - \sum_{i=I+1,m} (\beta_i - \alpha_i) K^i = \frac{1}{2}(U_L + U_R) + \frac{1}{2}\sum_{i=1,m} sign(\lambda_i)(\beta_i - \alpha_i) K^i$$

Thus, we can obtain the Godunov flux:

$$F(U(0)) = A(U(0)) = \frac{1}{2}(A(U_L) + A(U_R)) + \frac{1}{2}\sum_{i=1,m} sign(\lambda_i)(\beta_i - \alpha_i) A K^i$$

$$= \frac{1}{2}(F_L + F_R) + \frac{1}{2}\sum_{i=1,m} |\lambda_i|(\beta_i - \alpha_i) K^i$$
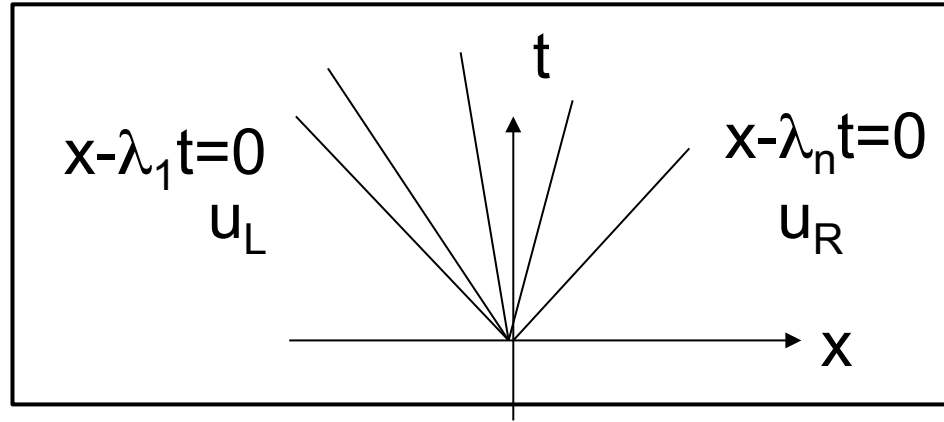
$$F = \frac{1}{2}(F_L + F_R) + \frac{1}{2}\sum_{i=1,m}|\lambda_i|(\beta_i - \alpha_i)K^i$$

Mean flux

Diffusive part ensuring upwinding and code stability

An example:

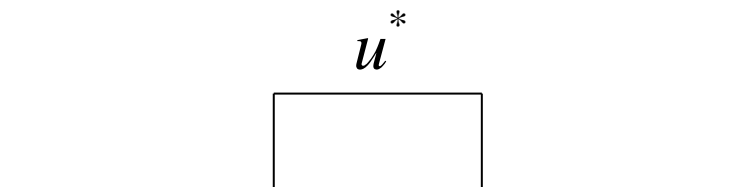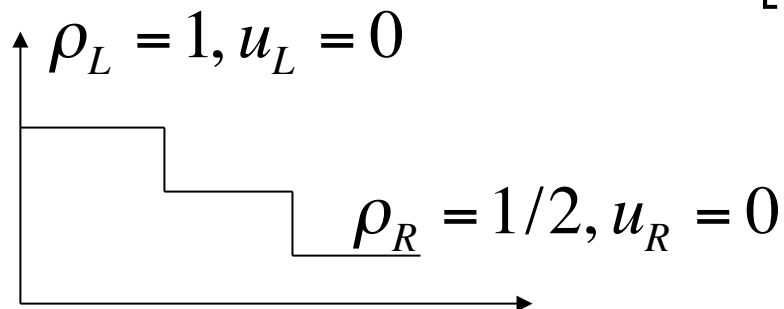Let us consider the linearized 1D hydrodynamical equations.

$$U_t + AU_x = 0,$$

$$U = \begin{bmatrix} u_1 \\ u_2 \end{bmatrix} = \begin{bmatrix} \rho \\ u \end{bmatrix}, A = \begin{bmatrix} 0 & \rho_0 \\ a^2/\rho_0 & 0 \end{bmatrix} \rightarrow \lambda_1 = -a, \lambda_2 = a, K^{(1)} = \begin{bmatrix} \rho_0 \\ -a \end{bmatrix}, K^{(2)} = \begin{bmatrix} \rho_0 \\ a \end{bmatrix}$$

$$U_L = \begin{bmatrix} \rho_L \\ u_L \end{bmatrix} = \alpha_1 K^{(1)} + \alpha_2 K^{(2)} \Rightarrow \alpha_1 = \frac{a\rho_L - \rho_0 u_L}{2a\rho_0}, \alpha_2 = \frac{a\rho_L + \rho_0 u_L}{2a\rho_0},$$

$$idem\,(\beta, R) \leftrightarrow (\alpha, L)$$

$$U^* = \begin{bmatrix} \rho^* \\ u^* \end{bmatrix} = \alpha_2 K^{(2)} + \beta_1 K^{(1)} = \begin{bmatrix} \frac{1}{2}(\rho_L + \rho_R) - \frac{1}{2}(u_R - u_L)\rho_0/a \\ \frac{1}{2}(u_L + u_R) - \frac{1}{2}(\rho_R - \rho_L)a/\rho_0 \end{bmatrix}$$

$$\rho_L = 1, u_L = 0$$

$$\rho_R = 1/2, u_R = 0$$

$$u^*$$

The ROE Riemann solver (MHD solver)

3 waves linear solver for HD (Roe 1981, Toro 1999).

7 waves linear solver for MHD (Brio & Wu 1988, Cargo & Gallice 1998, Balsara 1998).

Complex method which requires some calculations. Only the basic ideas presented here.

Solving the Riemann problem exactly is too difficult so one replaces the non linear problem by a linear problem that is solved *exactly*.

Replace the new Jacobian, A, by a linear one which has adequate properties.

$$\partial_t U + F(U)_x = 0, \partial_t U + A U_x = 0 \approx \partial_t U + \tilde{A} U_x = 0, \quad \tilde{A}(U_L, U_R)$$

It is required to have the following properties:

Property (A): Hyperbolicity of A, implying that it has m eigenvalues and eigenvectors. $\tilde{\lambda}_1 \leq ... \leq \tilde{\lambda}_m, \tilde{K}_1, ..., \tilde{K}_m,$

This preserves the linear wave structure of the original problem.

<u>Property (B):</u> $\tilde{A}(U,U) = A(U)$

This is called the *consistency*. It implies that in the limit where the right and left states becomes identical, the flux is exactly recovered.

<u>Property (C):</u> $\tilde{A}(U_R,U_L)(U_R - U_L) = F(U_R) - F(U_L)$

This is the most difficult property to satisfy.

It ensures that an isolated discontinuity which satisfies the jump relation:

$$F_R - F_L = \lambda_c(U_R - U_L)$$

will be adequatly described by the solver (projected in a single eigenvector giving $\lambda_c = \lambda_i$).

Constructing a Roe matrix is not easy. Simple averaging like $0.5(A(U_R) + A(U_L))$ does not verify property (C).

This can be achieved (Roe 1981) by introducing an intermediate vector Q.

$$U = U(Q), F = F(Q), Q = \sqrt{\rho}(1,u,v,w,H,B_y/\rho,B_z/\rho)$$

$$H = \frac{1}{\rho}\left(E + P + \frac{1}{2}\left(B_x^2 + B_y^2 + B_z^2\right)\right)$$

By doing this, it is found that U and F express as algebraic relations (product Q_iQ_j or ratio Q_i/Q_j) involving the components of Q.   But we have for example:

$$Q_{1,R}Q_{2,R} - Q_{1,L}Q_{2,L} = \Delta(Q_1Q_2) = \overline{Q}_2\Delta Q_1 - \overline{Q}_1\Delta Q_2$$

Thus the jump relations can be expressed by the jump relation of Q:

$$F_R - F_L = \Delta F = \tilde{C}\Delta Q, \quad (U_R - U_L) = \Delta U = \tilde{B}\Delta Q$$

Thus,
$$\tilde{A} = \tilde{C}\tilde{B}^{-1}, \quad F_R - F_L = \tilde{A}(U_R - U_L)$$

And the flux is given by the formula obtained previously:

$$F(U(0)) = \frac{1}{2}(F_L + F_R) + \frac{1}{2}\sum_{i=1,m}\left|\tilde{\lambda}_i\right|(\tilde{\beta}_i - \tilde{\alpha}_i)\tilde{K}^i$$

To summarize, the whole algorithm is:

-compute the Roe average, involved quantities like: $\tilde{u} = \dfrac{\sqrt{\tilde{\rho}_L}u_L + \sqrt{\tilde{\rho}_R}u_R}{\sqrt{\tilde{\rho}_L} + \sqrt{\tilde{\rho}_R}}$

-compute the eigenvalues and eigenvectors

-compute the wave strength ($\alpha{-}\beta$)

-compute the flux

Generally speaking, the Roe solver works well and gives accurate results. It is widely used and serves as a reference.

In some rare occasions (but not so rare….), the Roe solver is encountering severe difficulties and crashes.This is due to the linearisation which is a poor approximation for highly non linear discontinuities encountered in stiff problems.

The manifestation of this can be:

-intermediate states with negative energy or density

-rarefaction shocks leading to entropy violation

An entropy fix or more generally a switch is needed to cure these events… Various possibilities have been proposed (see e.g. Toro 1999).

For example, one can switch to HLL using the largest and smallest wave speed of Roe. This replaces the 6 intermediate Roe states by a single star state.
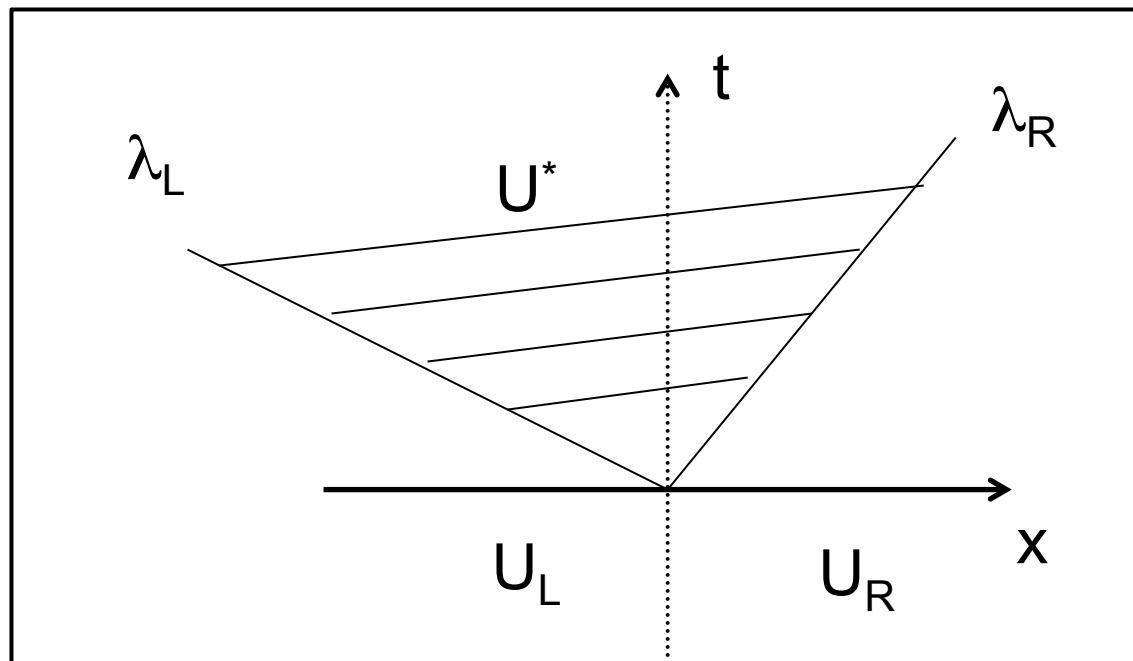
The H(arten)L(ax) (van)L(eer) Riemann solver

(Harten et al. 1983, Toro 1999)

2 waves solver (hydro and mhd):

one retains only the 2 fastest waves (e.g. the 2 fast magneto-accoustic waves) and then assume that between the 2 waves, there is a uniform state U*.

Conservation laws are then used to determine U* and the flux F *.

First step (HLL)

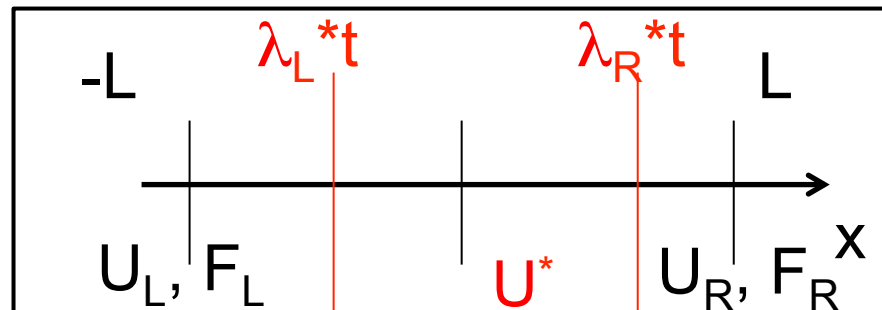Let us consider a volume of control V, i.e. an area of surface S in YZ and delimited by -L and L in X.

At time t=0, the total value of U within V is: $(S \times 2L) \times U_{tot} = S \times L \times (U_L + U_R)$

At time t, the left and the right waves have reached: $X = \lambda_L \times t, X = \lambda_R \times t$

Thus:
$$(S \times 2L) \times U_{tot}(t) =$$
$$S \times ((L + \lambda_L t) \times U_L + (L - \lambda_R t) \times U_R + (-\lambda_L + \lambda_R) t \times U^*)$$

But we also have: $(S \times 2L) \times (U_{tot}(t) - U_{tot}(0)) = (F_L - F_R) \times t$

Thus we obtain U*:
$$U^* = \frac{F_L - F_R + \lambda_R U_R - \lambda_L U_L}{\lambda_R - \lambda_L}$$

Second step (HLL)

But what we want, is to determine F*, so the job is not finished yet

(F(U*) is not a good solution). Assume first that: $\lambda_L < 0$, $\lambda_R > 0$

Let us consider a new volume of control, delimited by X=-L and X=0. Then we have:

$$S \times ((L + \lambda_L t) \times U_L - \lambda_L t \times U^*) = SL \times U_L + (F_L - F^*)t$$

and thus:

$$F^* = F_L + \lambda_L (U^* - U_L) = \frac{\lambda_R F_L - \lambda_L F_R + \lambda_L \lambda_R (U_R - U_L)}{\lambda_R - \lambda_L}$$

Note that this expression is symmetrical in R <=> L indicating that we could have used X=0, X=L as volume of control and find the same result.

If now we assume that: $\lambda_L > 0$, $\lambda_R > 0$, that is to say the left state propagates faster than the fastest wave in the right direction, the same calculation shows that $F_{HLL} = F_L$. In the same way $\lambda_L < 0$, $\lambda_R < 0$ implies $F_{HLL} = F_R$

$$\lambda_L < 0, \lambda_R > 0 \rightarrow F_{HLL} = F^* = \frac{\lambda_R F_L - \lambda_L F_R + \lambda_L \lambda_R (U_R - U_L)}{\lambda_R - \lambda_L}$$

$$\lambda_L > 0, \lambda_R > 0 \rightarrow F_{HLL} = F_L$$

$$\lambda_L < 0, \lambda_R < 0 \rightarrow F_{HLL} = F_R$$

$$Note\ that: \quad F_L \rightarrow F^* \ when \ \lambda_L \rightarrow 0$$

Which wave speed ?

In principle, determining the correct wave speeds would require to solve the problem exactly first… Fortunately, good estimates can be made.

Davis (1988) propose:

$$S_L = \min[\lambda_l(U_L), \lambda_l(U_R)]$$
$$S_R = \max[\lambda_m(U_L), \lambda_m(U_R)]$$

while Einfeldt et al. (1991) propose:

$$S_L = \min[\lambda_l(U_L), \lambda_l(U_{Roe})]$$
$$S_R = \max[\lambda_m(U_L), \lambda_m(U_{Roe})]$$

where λ_l and λ_m are respectively the smallest and largest wave speeds and λ_{roe} are the Roe wave speeds.

Positivity of the scheme

In the hydrodynamical case, the scheme ensures positivity that is to say, density and pressure remain positive (Einfeldt et al. 1991). The common experience is that the scheme is very robust.

However, the scheme does not resolve contact discontinuities and is therefore very diffusive. Single-state approximation should be extended to a two or multi-state approximation.

Note when $\lambda_L = \lambda_R$ is enforced, the scheme is called Lax-Friedrich solver.

The HLLC Riemann solver (hydro case)

3 waves solver (Toro 1999):

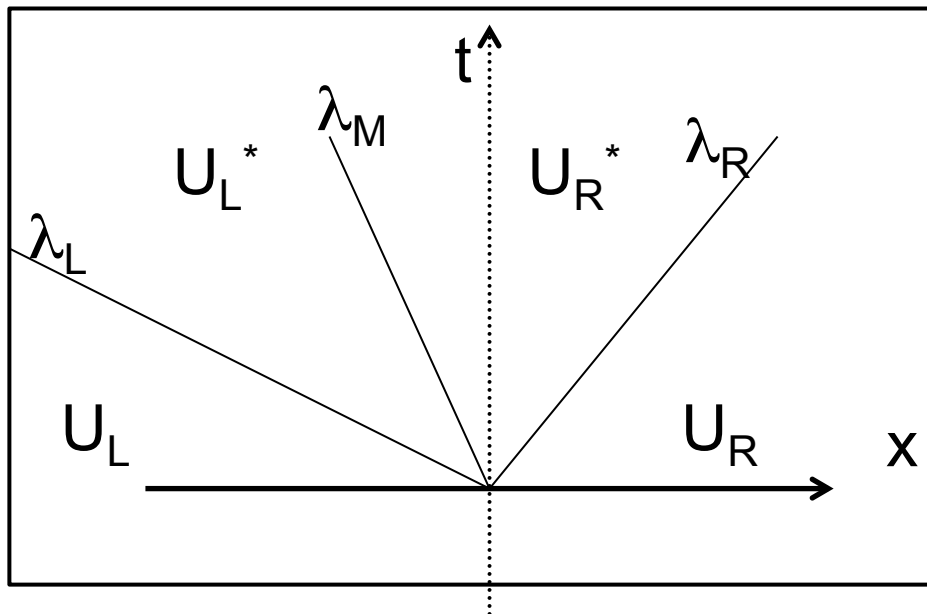2 fast waves and 1 entropy wave. Thus, 2 intermediate states U_L* and U_R*.

First step (HLLC)

It is assumed that the normal velocity is constant over the Riemann fan, thus, the wave velocity of the entropy wave is

$$\lambda_M = u_L^* = u_R^*$$

Second step (HLLC)

λ_M, or equivalently, u* has to be guessed. Since u is the same in the 2 states a good choice is:

$$\lambda_M = u_L^* = u_R^* = \frac{(\rho u)^*}{\rho^*} =$$

$$\frac{(\lambda_R - u_R)\rho_R u_R - (\lambda_L - u_L)\rho_L u_L - P_R + P_L}{(\lambda_R - u_R)\rho_R - (\lambda_L - u_L)\rho_L}$$

Third step (HLLC)

We need to determine the remaining quantities in the two star states.
We apply the jump conditions across the left and right waves, λ_L, λ_R:

$$\lambda_L U_L - F_L = \lambda_L U_L^* - F_L^*$$

$$\lambda_R U_R - F_R = \lambda_R U_R^* - F_R^*$$

Thus, we obtain the pressure P* (use expression of λ_M to show that $P_L^* = P_R^*$):

$$P^* = P_\alpha^* = P_\alpha + \rho_\alpha(\lambda_\alpha - u_\alpha)(\lambda_M - u_\alpha)$$

and the other quantities: $\rho_\alpha^* = \rho_\alpha \dfrac{\lambda_\alpha - u_\alpha}{\lambda_\alpha - \lambda_M}$

$$v_\alpha^* = v_\alpha$$

$$w_\alpha^* = w_\alpha$$

$$e_\alpha^* = \frac{(\lambda_\alpha - u_\alpha)e_\alpha - P_\alpha u_\alpha + P^*\lambda_M}{\lambda_\alpha - \lambda_M}$$

where α=L or R

Fourth step (HLLC)

We need to determine the flux used to update U_L and U_R. We proceed as for HLL.

$$\lambda_L < 0, \lambda_M > 0 \rightarrow F_{HLLC} = \frac{\lambda_M F_L - \lambda_L F_L^* + \lambda_L \lambda_M (U_L^* - U_L)}{\lambda_M - \lambda_L}$$

$$\lambda_R > 0, \lambda_M < 0 \rightarrow F_{HLLC} = \frac{\lambda_R F_R^* - \lambda_M F_R + \lambda_R \lambda_M (U_R - U_R^*)}{\lambda_R - \lambda_M}$$

$$\lambda_L > 0, \lambda_R > 0 \rightarrow F_{HLLC} = F_L$$

$$\lambda_L < 0, \lambda_R < 0 \rightarrow F_{HLLC} = F_R$$

Note again the continuity of the flux since for example:

$$F_{HLLC} \rightarrow F_L^* \rightarrow F_R^* \quad when \quad \lambda_M \rightarrow 0$$

Batten et al. (1997) show that the HLLC solver is positively conservative if the wave speeds are as indicated previously.

This solver can resolve contact discontinuities. It is therefore less diffusive than HLL. Can we generalise it to MHD ?
Since, contrarily to HLL, HLLC uses jump conditions, generalisation is not at all straightforward.

Problem in generalising HLLC to MHD

Gurski (2004), Linde (2002)

In the case Bx = 0, HLLC can be generalised (no Alfven wave in this case). However, in the general case Bx is not zero and Alfven waves propagate.

The jump conditions across the 2 fast waves are not compatible with the jump conditions across the contact discontinuity.

This leads to problems:
-the solver cannot resolve well Alfven waves and slow waves.
-attempt to improve this, leads to unphysical oscillations

The problem is that there is not enough degrees of freedom with 2 states to describe one entropy wave and 2 Alfven waves.

The HLLD Riemann solver (MHD solver)

5 waves solver (Miyoshi & Kusano 2005):

2 fast waves, 2 Alfvén waves and 1 entropy wave. Thus, 4 intermediate states U_L^*, U_L^{**} and U_R^*, U_R^{**}.
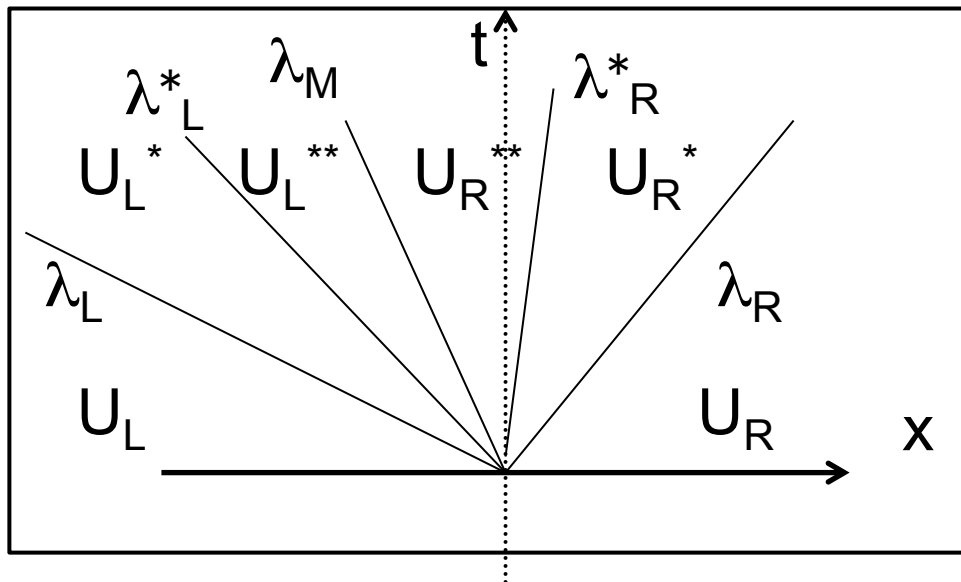
First step (HLLD)

assumed that the normal velocity is constant over the Riemann fan, thus, the wave velocity of the entropy wave is

$$\lambda_M = u_L^* = u_R^* = u_L^{**} = u_R^{**}$$

Second step (HLLD)

λ_M or equivalently, u* has to be guessed. As for HLLC:

$$\lambda_M = u_L^* = u_R^* = u_L^{**} = u_R^{**} = \frac{(\rho u)^*}{\rho^*} =$$

$$\frac{(\lambda_R - u_R)\rho_R u_R - (\lambda_L - u_L)\rho_L u_L - P_R + P_L}{(\lambda_R - u_R)\rho_R - (\lambda_L - u_L)\rho_L}$$

Third step (HLLD)

Determine all quantities in the two star states by applying the jump conditions across the left and right waves, λ_L, λ_R:

$$\lambda_\alpha U_\alpha - F_\alpha = \lambda_\alpha U_\alpha^* - F_\alpha^*$$

As for HLLC, the pressure P* (use expression of λ_M to show that $P_L^* = P_R^*$):

$$P^* = P_\alpha^* = \frac{\rho_R P_{T_L}(\lambda_R - u_R) - \rho_L P_{T_R}(\lambda_L - u_L) + \rho_L \rho_R (\lambda_R - u_R)(\lambda_L - u_L)(u_R - u_L)}{\rho_R(\lambda_R - u_R) - \rho_L(\lambda_L - u_L)}$$

and the other quantities:

$$\rho_\alpha^* = \rho_\alpha \frac{\lambda_\alpha - u_\alpha}{\lambda_\alpha - \lambda_M}$$

$$v_\alpha^* = v_\alpha - B_x B_{y\alpha} \frac{\lambda_M - u_\alpha}{\rho_\alpha(\lambda_\alpha - u_\alpha)(\lambda_\alpha - \lambda_M) - B_x^2}$$

$$B_{y\alpha}^* = B_{y\alpha} \frac{\rho_\alpha(\lambda_\alpha - u_\alpha)^2 - B_x^2}{\rho_\alpha(\lambda_\alpha - u_\alpha)(\lambda_\alpha - \lambda_M) - B_x^2}$$

same for w and B_z

where α=L or R

$$e_\alpha^* = \frac{(\lambda_\alpha - u_\alpha)e_\alpha - P_{T_\alpha} u_\alpha + P_T^* \lambda_M + B_x(\vec{V}_\alpha . \vec{B}_\alpha - \vec{V}_\alpha^* . \vec{B}_\alpha^*)}{\lambda_\alpha - \lambda_M}$$

Fourth step (HLLD)

Determine *some* quantities in the two star states by applying the jump conditions across the two left and right star waves, λ_L^*, λ_R^*:

$$\lambda_\alpha^* U_\alpha^* - F_\alpha^* = \lambda_\alpha^* U_\alpha^{**} - F_\alpha^{**}$$

Since normal velocity is constant through the fan, $\lambda_M = u_L^* = u_R^* = u_L^{**} = u_R^{**}$ for any wavelength such that $\lambda_L < \lambda < \lambda_M$ or $\lambda_M < \lambda < \lambda_R$, the density and pressure are constant (star wave are alfvén waves)

$$\rho_\alpha^* = \rho_\alpha^{**} , P_{T_\alpha}^* = P_{T_\alpha}^{**}$$

Fifth step (HLLD)

Determine the wave speed λ_L^*, λ_R^*. Since these are Alfvén waves, it seems appropriate to choose:

$$\lambda_L^* = \lambda_M - \frac{|B_x|}{\sqrt{\rho_L^*}} , u_R^* = \lambda_M + \frac{|B_x|}{\sqrt{\rho_L^*}}$$

Sixth step (HLLD)

Apply jump conditions through the contact discontinuity. This shows that transverse v, w, B_y and B_z are constant (as expected for a contact discontinuity).

$$v_\alpha^{**} = v^{**} , B_{y_\alpha}^{**} = B_y^{**} , w_\alpha^{**} = w^{**} , B_{z_\alpha}^{**} = B_z^{**}$$

Seventh step (HLLD)

Determine, v^{**}, w^{**}, B_y^{**}, B_z^{**}

For this purpose, use conservation within the volume of control as for HLL but with 5 waves instead of 2.

$$(\lambda_R - \lambda_R^*)U_R^* + (\lambda_R^* - \lambda_M)U_R^{**} + (\lambda_M - \lambda_L^*)U_L^{**} + (\lambda_L^* - \lambda_L)U_L^* - \lambda_R U_R + \lambda_L U_L$$

$$-F_L + F_R = 0$$

This leads to:

$$v^{**} = \frac{\sqrt{\rho_L^*}\,v_L^* + \sqrt{\rho_R^*}\,v_R^* + (B_{y_R}^* - B_{y_L}^*)sign(B_x)}{\sqrt{\rho_L^*} + \sqrt{\rho_R^*}}$$

$$B_y^{**} = \frac{\sqrt{\rho_L^*}\,B_{y_L}^* + \sqrt{\rho_R^*}\,B_{y_R}^* + (v_R^* - v_L^*)sign(B_x)}{\sqrt{\rho_L^*} + \sqrt{\rho_R^*}}$$

Eighth step (HLLD):

Now compute the flux by using volume of control centered on X=0.
Since more star states, flux are slightly more complex than with HLL.

$$F_L^* = F_L + \lambda_L (U_L^* - U_L) \ if \ \lambda_L^* > 0$$

$$F_L^{**} = F_L + \lambda_L (U_L^* - U_L) + \lambda_L^* (U_L^{**} - U_L^*) \ if \ \lambda_L^* < 0 < \lambda_M$$

The flux is then:

$$\lambda_L > 0 \rightarrow F_{HLLD} = F_L$$

$$\lambda_L < 0 < \lambda_L^* \rightarrow F_{HLLD} = F_L^*$$

$$\lambda_L^* < 0 < \lambda_M \rightarrow F_{HLLD} = F_L^{**}$$

$$\lambda_M < 0 < \lambda_R^* \rightarrow F_{HLLD} = F_R^{**}$$

$$\lambda_R^* < 0 < \lambda_R \rightarrow F_{HLLD} = F_R^*$$

$$\lambda_R < 0 \rightarrow F_{HLLD} = F_R$$

Final remarks about HLLD:

The solver can resolve exactly isolated discontinuities including rotational discontinuities (Alfvén waves) and shocks.

As expected it does not resolve well slow magneto-accoustic waves.

Miyoshi & Kusano show that it preserves positivity.

It is a non-linear relatively accurate and robust solver.
=> Tends to be widely used.

HIGH ORDER SCHEMES

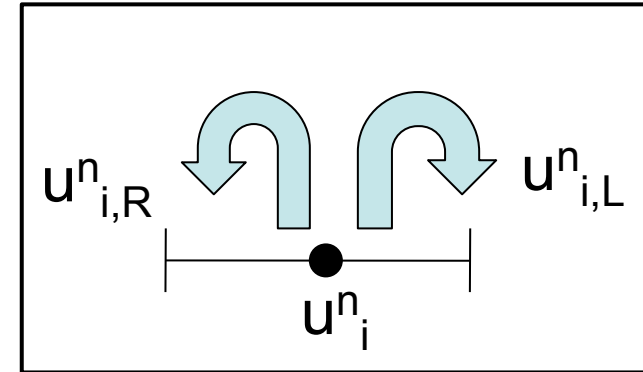# accuracy versus stability

The MUSCL-Hancock scheme

The Monotonic Upstream Centred
Scheme
for Conservation Laws

So far, the method was first order since each cell is described by a constant value. First order methods are very diffusive.

How to increase the order of the method ?

Replace the uniform state by a gradient => increase the order of the method.

Necessary to compute: $u^n_{i,L} = u^n_{i-1/2}$ and $u^n_{i,R} = u^n_{i+1/2}$

It is necessary also, to be in second order in times to compute these values a time $t+1/2\Delta t$

$$F^{n+1/2}_{i+1/2} = \frac{1}{\Delta t} \int_{t^n}^{t^{n+1}} F(U(x_{i+1/2}, t)) dt$$

$$\approx F(U^{n+1/2}_{i+1/2})$$
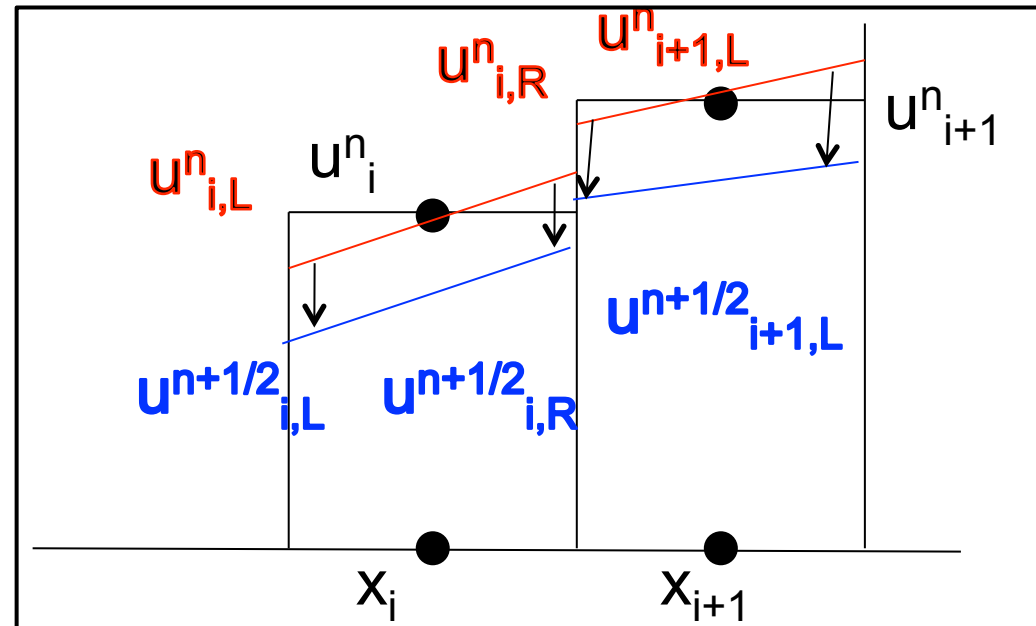
The Muscl-Handock scheme

The predictor states are calculated using Taylor expansion:

$$U_{i+1/2,L}^{n+1/2} \approx U_i^n + \frac{\Delta t}{2}\left(\frac{\partial U}{\partial t}\right)_i + \frac{\Delta x}{2}\left(\frac{\partial U}{\partial x}\right)_i$$

$$U_{i+1/2,R}^{n+1/2} \approx U_i^n + \frac{\Delta t}{2}\left(\frac{\partial U}{\partial t}\right)_i - \frac{\Delta x}{2}\left(\frac{\partial U}{\partial x}\right)_i$$

The time derivative is estimated by calculating the fluxes at time t^n.

The space derivatives are computed using the neighbours (but some difficulties will appear soon…).

Summary of the scheme:

-compute the boundary extrapolated values

-evolve them at time $\Delta t/2$

-solve the Riemann fluxes

-update the variables using the fluxes

Problem with the reconstruction:
High order (>2) linear methods are not monotone (Godunov theorem)

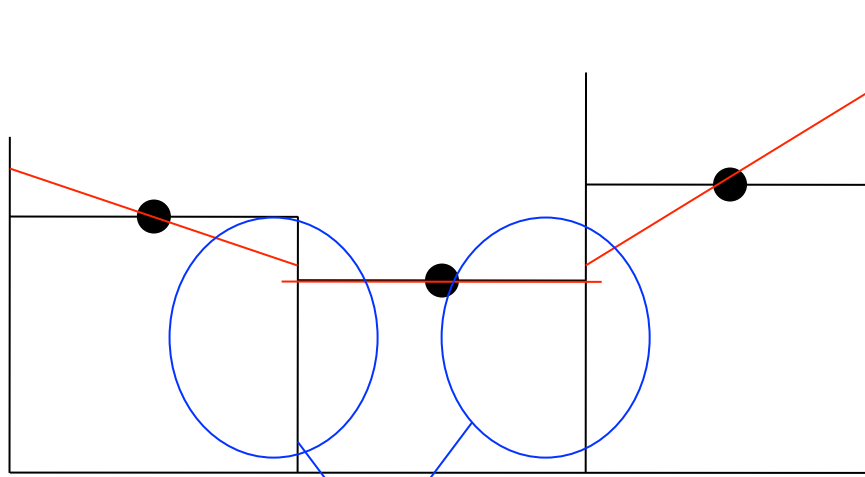$\Rightarrow$ Spurious numerical oscillations and instabilities in the vicinity of gradients.
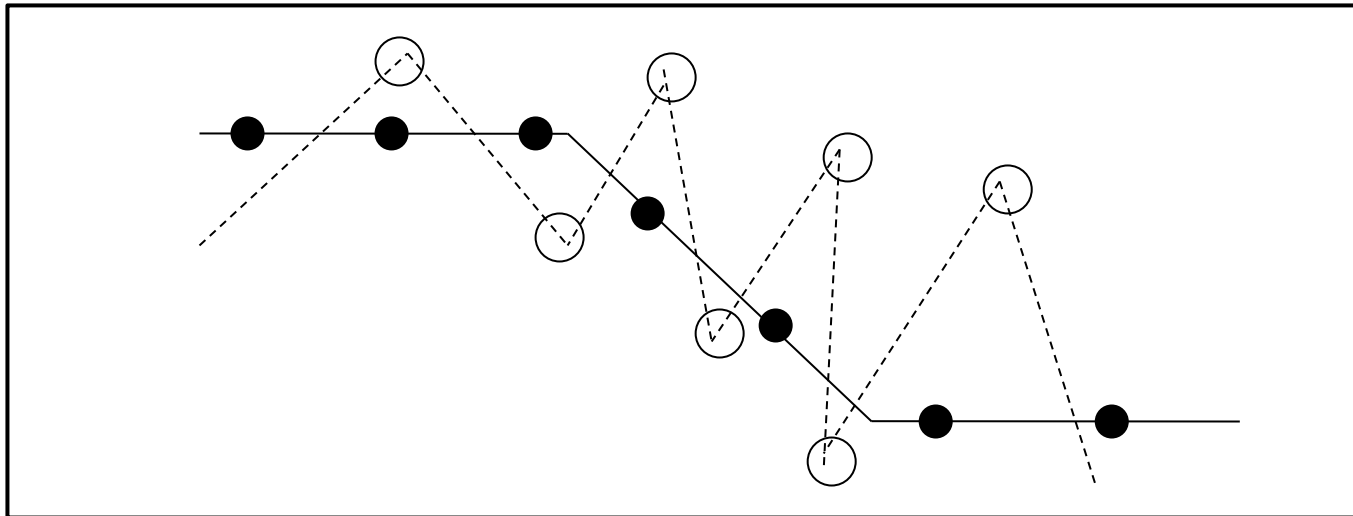
This implies that the slope must be adequately chosen. In particular, it must satisfy the TVD (Total Variation Diminishing) constraint.

Total Variation:

$$TV(u) = \int_{-\infty}^{\infty} |u'(x)| dx \Rightarrow TV(u_n) = \sum_{i=-\infty}^{\infty} |u_{i+1}^n - u_i^n|$$
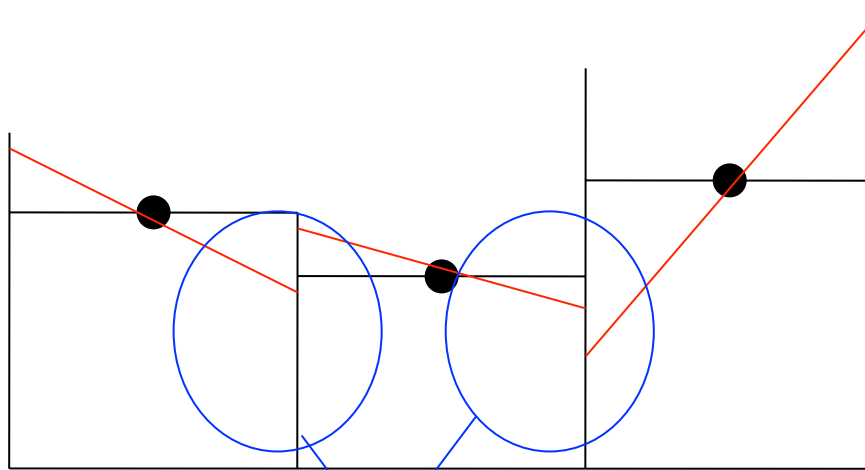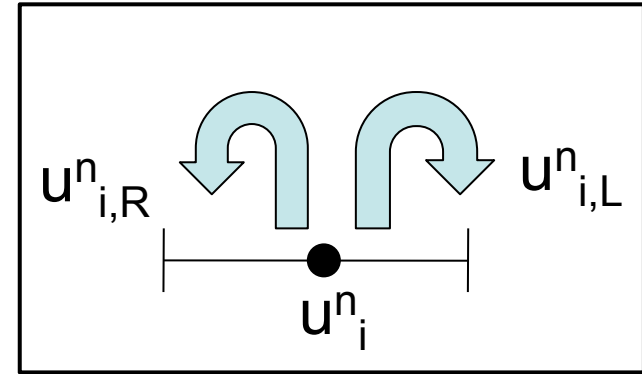
Local extremum=>non TVD

No local extremum=>TVD

Solution: use non-linear slope (slope limiter)

Generally speaking, we have:

$$u_{i,L}^{n} = u_i^{n} + \frac{1}{2}\Delta_i, u_{i,R}^{n} = u_i^{n} - \frac{1}{2}\Delta_i$$

$u_{i,R}^{n}$ $u_{i,L}^{n}$ u_i^{n}

Many slopes Δ_i can be constructed.

$$\Delta_{i,L} = u_i^{n} - u_{i-1}^{n}, \Delta_{i,R} = u_{i+1}^{n} - u_i^{n}, \Delta_{i,C} = (u_{i+1}^{n} - u_{i-1}^{n})/2$$

$$\Delta_i = f(\Delta_{i,L}, \Delta_{i,R}, \Delta_{i,C})$$

A very useful, widely used choice is the MINMOD slope:

$$\begin{cases} \Delta_L > 0, & \Delta_i = \max\left[0, \min(\Delta_{i,L}, \Delta_{i,R})\right] \\ \Delta_L < 0, & \Delta_i = \min\left[0, \max(\Delta_{i,L}, \Delta_{i,R})\right] \end{cases}$$

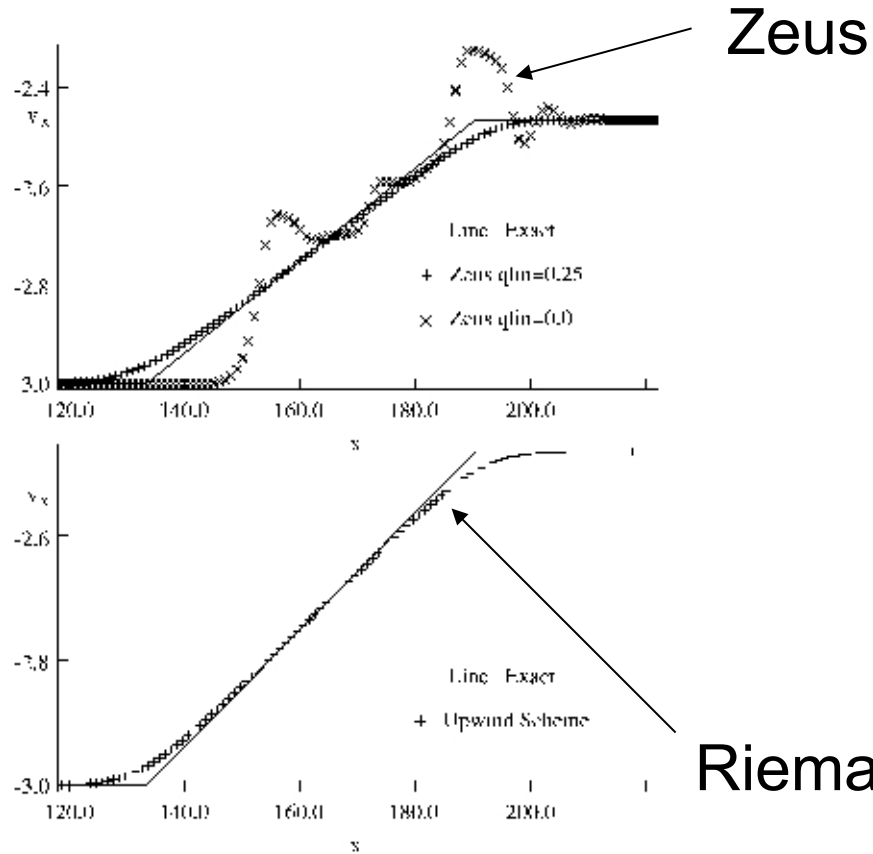Robust but diffusive (i.e. not very accurate)

In general, slopes are an important issue. Better to test various choices.

TESTING the SCHEME

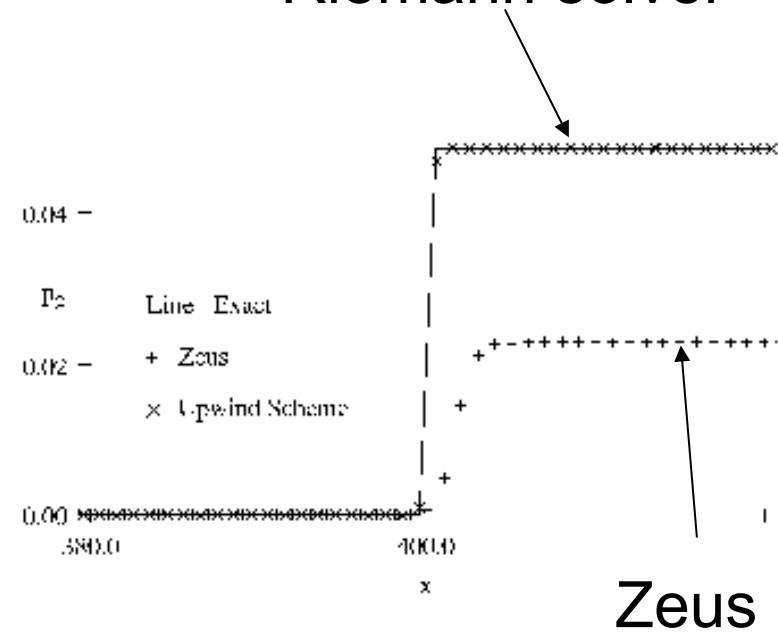**Importance of code testing cannot be over-emphasized…**

Have we wasted our time ?

Rarefaction shock

Inacurate Jump conditions

Zeus

Riemann solver

Riemann solver

Zeus

Falle 2002

Maybe not…

1D Tests for MHD

The non-linear circularly polarized Alfvén wave

(e.g. Fromang et al. 2006)

This is an exact and explicit solution

of MHD equation

=>very convenient to test the codes

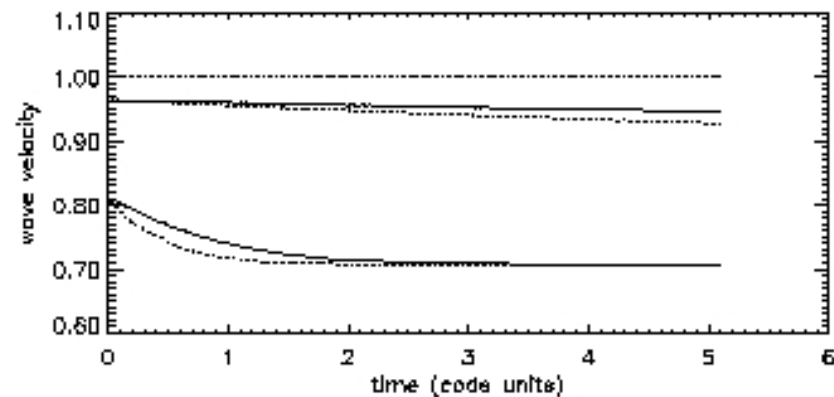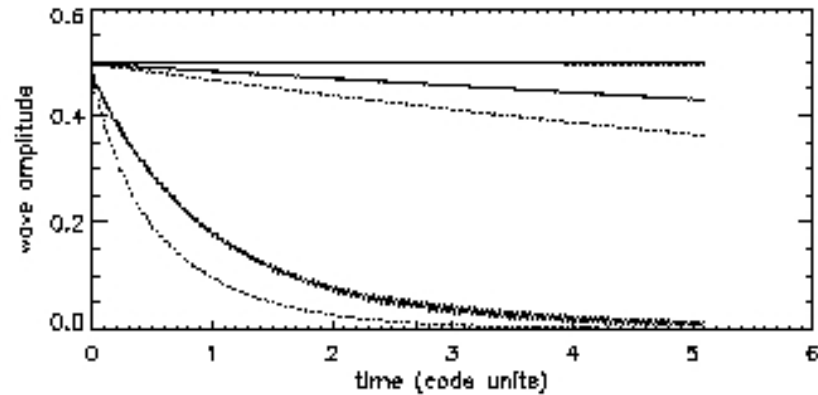Can be written as:

$$B_x = cst, V_x = 0,$$

$$V_y = A \times V_a \cos(\omega t - kx),$$

$$B_y = A \times B_x \cos(\omega t - kx),$$

$$V_z = A \times V_a \sin(\omega t - kx),$$

$$B_z = A \times B_x \sin(\omega t - kx),$$

$$\frac{\omega}{k} = V_a$$

1D Tests for MHD: Shock tube tests

Miyoshi & Kuzano 2005

Comparison between

HLL, ROE, HLLD

2 fast shocks (fast waves)

2 Alfven waves

2 slow waves

1 entropy wave

The 3 solvers do equaly well
for the fast waves
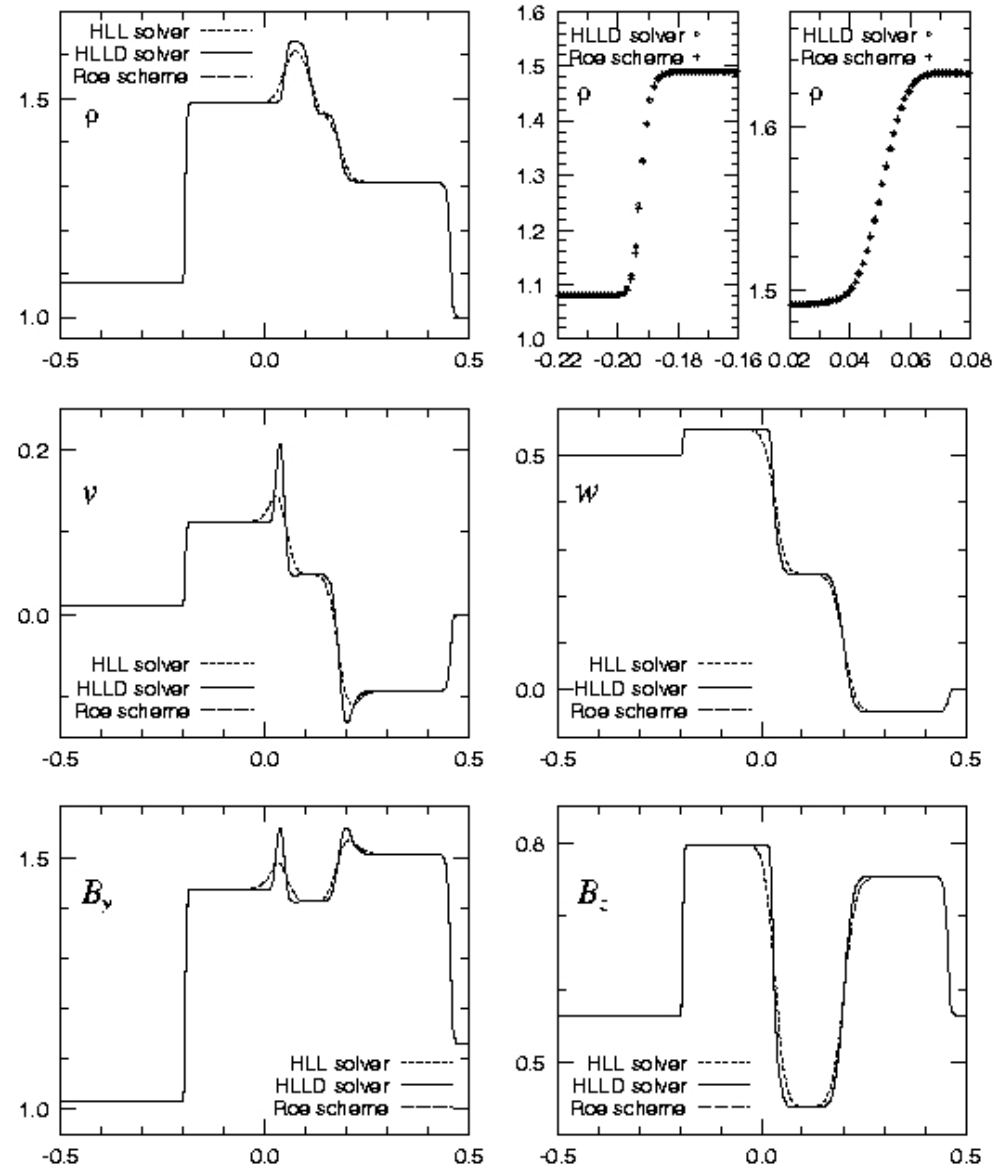
Roe and HLLD do better than

HLL for the other waves

Fig. 5. Results of one-dimensional shock tube test with the initial left states $(p, \rho, u, v, w, B_y, B_z) = (1.08, 0.95, 1.2, 0.01, 0.5, 3.6/\sqrt{4\pi}, 2/\sqrt{4\pi})$, the right states $(1, 1, 0, 0, 0, 0.4/\sqrt{4\pi}, 2/\sqrt{4\pi})$, and $B_x = 4/\sqrt{4\pi}$. Numerical solutions of the HLL solver, the HLLD solver, and the Roe scheme are plotted at $t = 0.2$. (Top left) p, (middle left) v, (middle right) w, (bottom left) B_y, (bottom right) B_z, (top middle) ρ around the left fast shock, (top right) ρ around the left slow shock are shown.

1D Tests for MHD: Shock tube tests

Influence of the
scheme order

HLLD first and
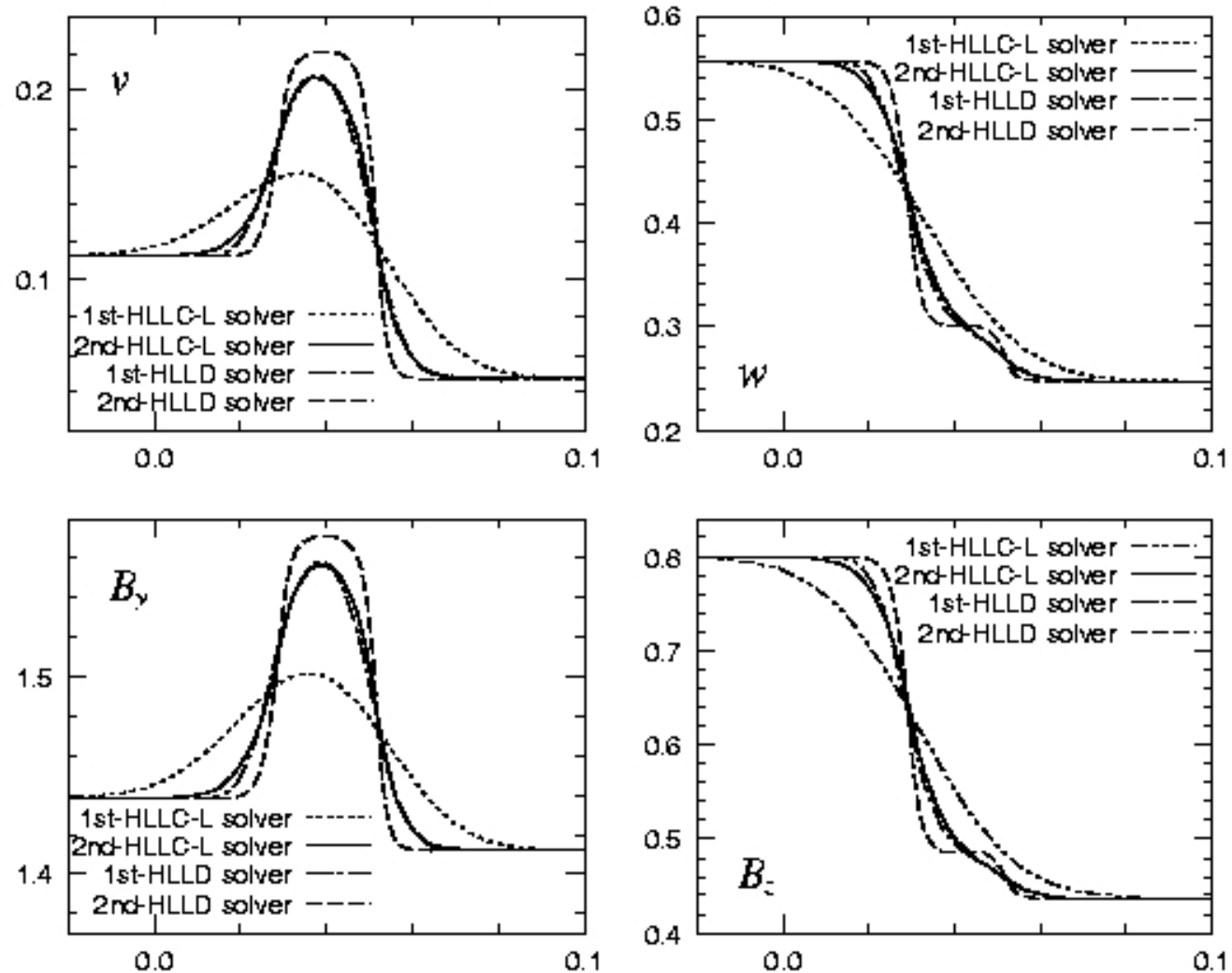second order

HLLC first and
second order

Fig. 7. Results of one-dimensional shock tube test with the same initial states as in Fig. 5. Numerical solutions of the first- and second-order HLLC-type solver by Li (1st- and 2nd-HLLC-L) [19], the first- and second-order HLLD solver (1st- and 2nd-HLLD) are plotted at $t = 0.2$. (Top left) v, (top right) w, (bottom left) B_y, (bottom right) B_z are shown within $-0.02 < x < 0.1$.

2D Tests for MHD: Orszag-Tang vortex test

Famous 2D tests

$$\rho = \gamma P_0,$$
$$v = (-\sin 2\pi y, \sin 2\pi x),$$
$$B = (-B_0 \sin 2\pi x, \sin 4\pi y)$$
$$\gamma = \frac{5}{3}, P_0 = \frac{5}{12\pi}, B_0 = \frac{1}{\sqrt{4\pi}}$$
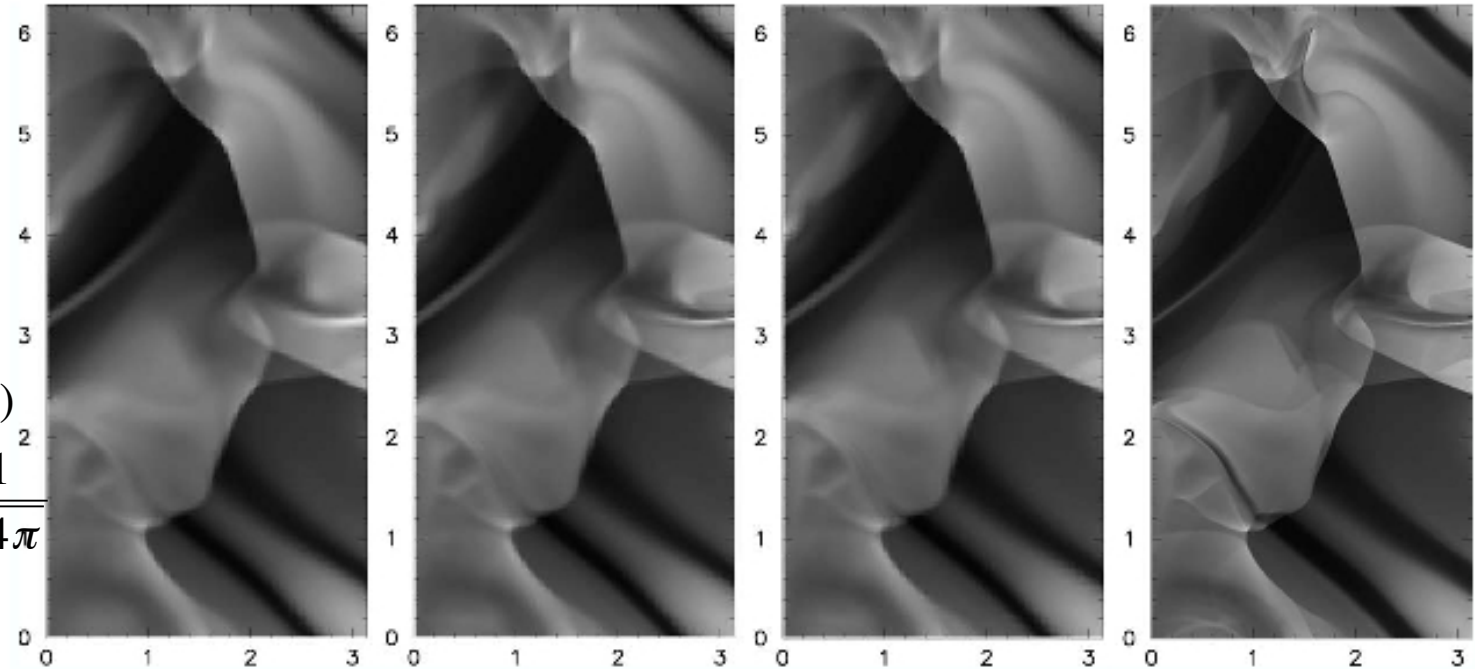
Fig. 12. Gray-scale images of the temperature distribution in the Orszag–Tang vortex problem at $t = \pi$ for (left to right) the **HLL** solver, the **HLLD** solver, the Roe scheme at $N = 200$, and the reference solution. The left half of the domain is shown.
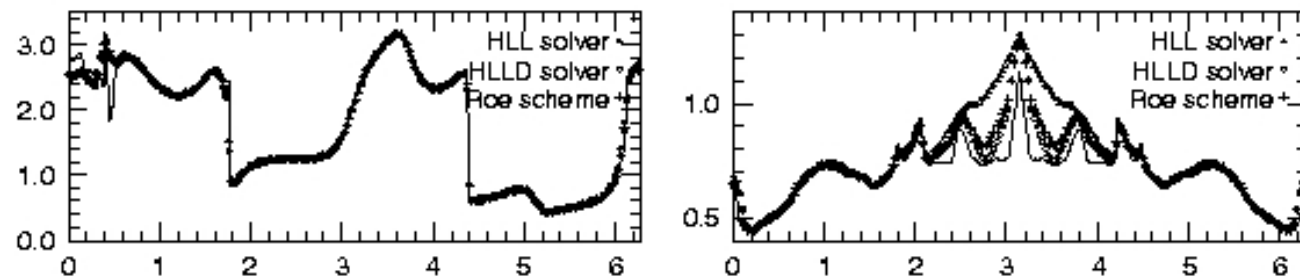
Comparison between HLL, HLLD and ROE

Fig. 13. One-dimensional temperature distribution in the same problem as in Fig. 12 along (left) $y = 0.64\pi$, (right) $y = \pi$, for the **HLL** solver, the **HLLD** solver, and the Roe scheme. The solid line shows the reference solution in each panel.

An exemple of a 3D calculation:

Collapse of a prestellar dense core with Lax-Friedrich solver
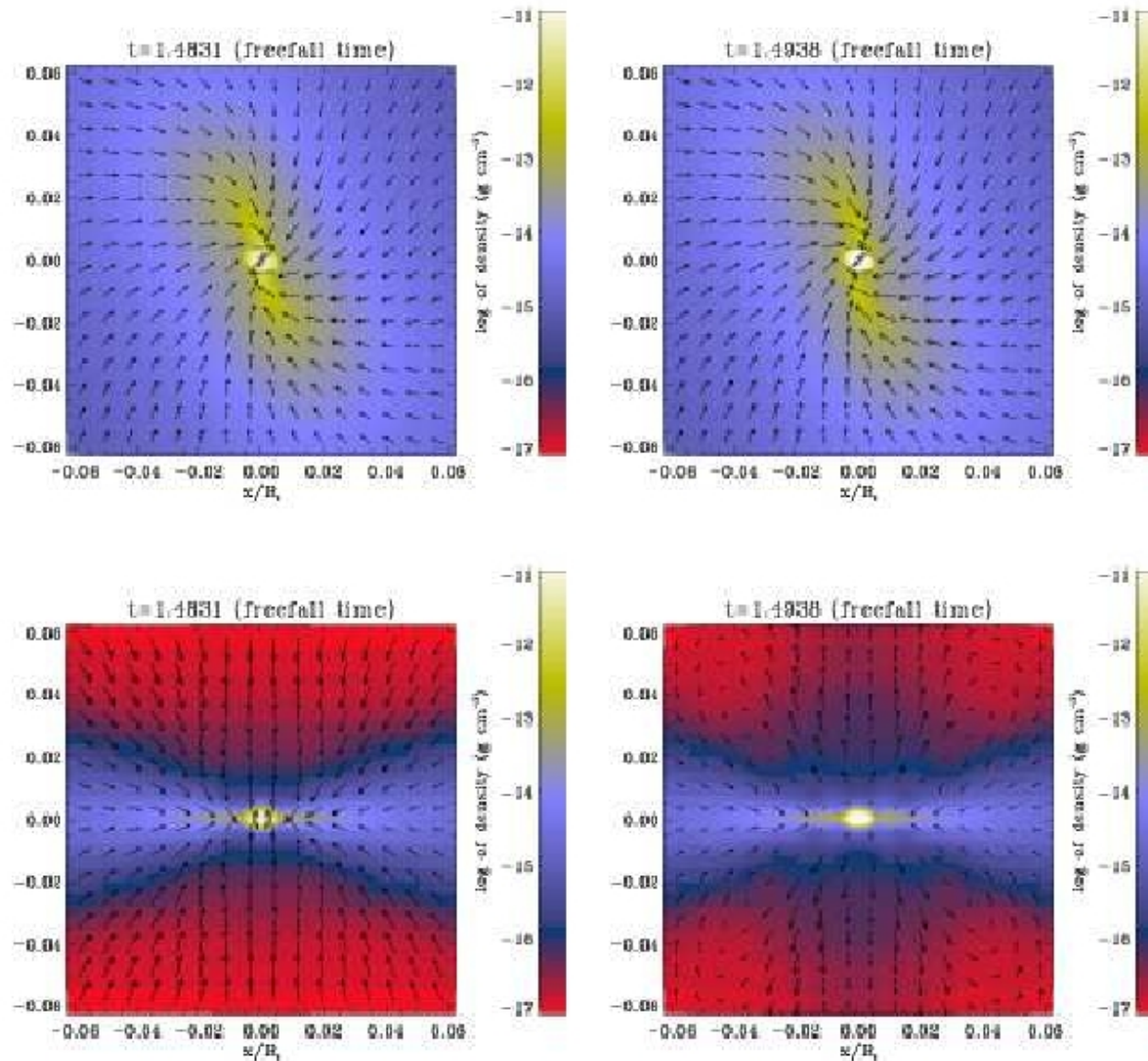
Fig. 13. Two timesteps illustrating the magnetized collapse. The upper panels display the equatorial density and velocity field whereas bottom panels displays the density in $x - z$ plan. The calculation is performed with the Lax-Friedrich solver.

An exemple of a 3D calculation:

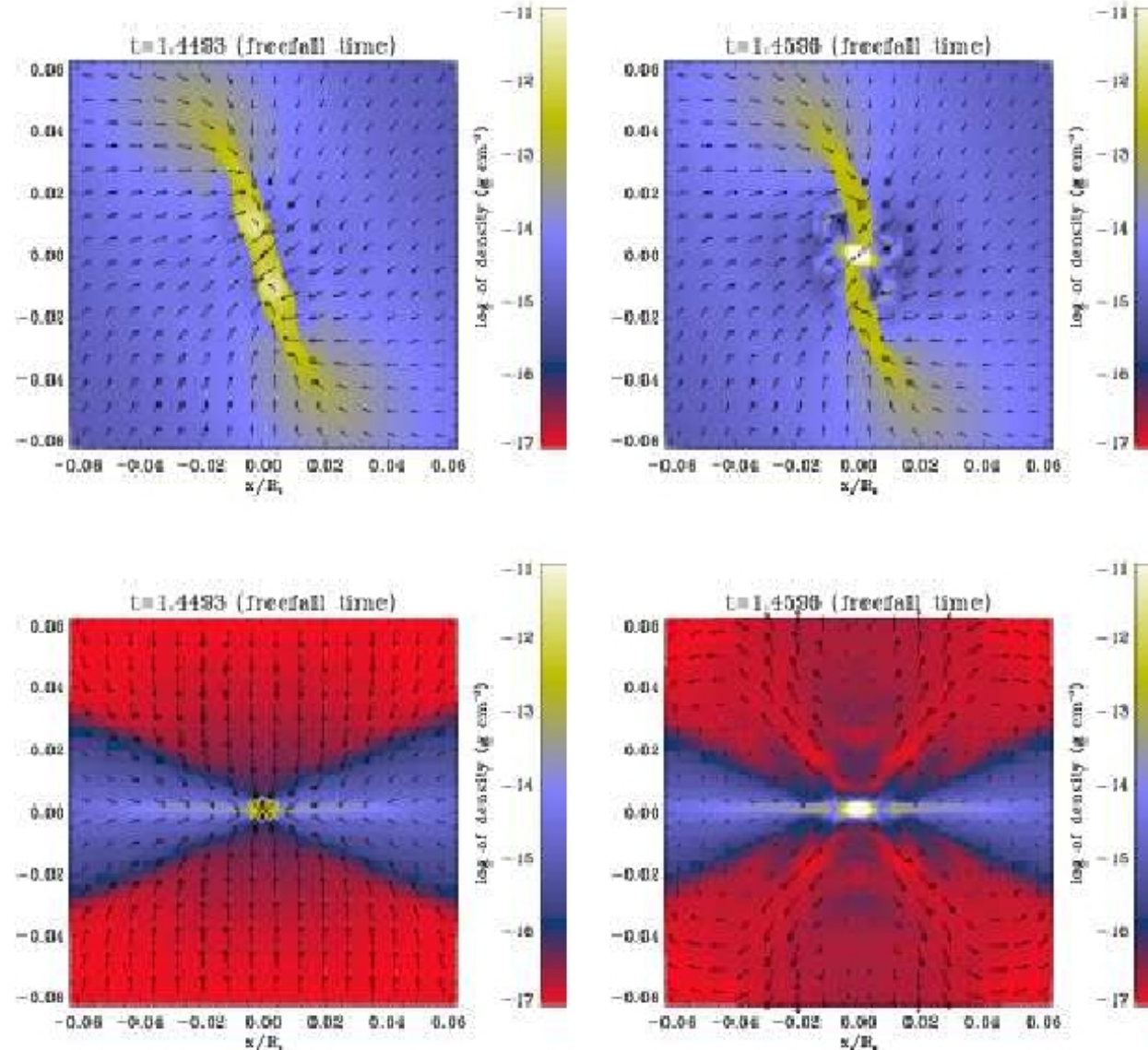## Collapse of a prestellar dense core with Roe solver

Fig. 14. Same as Fig. 13 except that the calculation has been carried out with the Roe solver.

MultiD-MHD

Specificity of the multiD MHD equations

In multidimensionnal problems, the induction equation presents qualitatively new features. Let us remember that the two following equations must be satisfied:

$$\partial_t \vec{B} + \vec{\nabla} \times (\vec{B} \times \vec{V}) = 0$$

$$\vec{\nabla}.\vec{B} = 0$$

Let us consider a surface S. Stokes theorem leads to:

$$\iint \partial_t \vec{B}.d\vec{S} + \iint \vec{\nabla} \times (\vec{B} \times \vec{V})).d\vec{S} = 0$$

$$\partial_t \phi + \oint (\vec{B} \times \vec{V}).d\vec{l} = 0$$

which is qualitatively different from mass, energy that are volume conserved…
The magnetic flux is defined on a surface rather than on a volume
=> *apparently* **difficulty to reconcile with Godunov-type methods**.

If div B, vanishes initially, induction equation ensures that it remains 0.

$$\vec{\nabla}.(\partial_t \vec{B} + \vec{\nabla} \times (\vec{B} \times \vec{V})) = 0$$

$$\Rightarrow \partial_t (\vec{\nabla}.\vec{B}) = 0$$

BUT: the numerical scheme, usually, will not ensure that this is the case.

Why worrying about div B=0 ?

(e.g. Brackbill & Barnes 1980, Toth 2000).
In numerical approaches, all quantities are always represented approximately, so why should we worry about div B being none zero as long as it remains small ?
The problem appears to be fundamental. Indeed, MHD equations on the conservative can be rewritten as:

$$\partial_t(\rho\vec{V}) + \vec{\nabla}(\rho\vec{V}\vec{V} - \vec{B}\vec{B} + P_{tot}I) = -\vec{\nabla}.\vec{B}\,\vec{B}$$

$$\partial_t E + \vec{\nabla}.((E + P)\vec{V} - \vec{B}(\vec{B}.\vec{V})) = -\vec{\nabla}.\vec{B}\,(\vec{V}.\vec{B})$$

Thus, if div B is not vanishing, the equations written on the conservative form are not equivalent to the standard fluid equations. In particular, we see that a force along the field lines is now applying.
Long time integration can then be a worry. Equilibrium solutions can be modified. For example Brackbill & Barnes report problems with integration of a uniform low beta plasma. After several crossing times, non zero flow velocities develop spontaneously and distort the field lines. The problem may be less severe if we use non conservative form of the MHD equations but then the nice properties of Godunov type schemes are lost.

The common experience is that non div B preserving schemes are very unstable and lead to code crashes.

Potential vector methods

(e.g. Dorfi 1986, Evans & Hawley 1988). B is volume centered.

Vector potential defined by:

$$\vec{\nabla} \times \vec{A} = \vec{B}$$

$$Thus : \vec{\nabla} . \vec{B} = \vec{\nabla} . (\vec{\nabla} \times \vec{A}) = 0$$

div B is therefore 0 exactly. On the other hand, the Lorentz force becomes:

$$\vec{j} \times \vec{B} = (\vec{\nabla} \times \vec{B}) \times \vec{B} = (\vec{\nabla} \times (\vec{\nabla} \times \vec{A})) \times (\vec{\nabla} \times \vec{A})$$

Therefore, the Lorentz force entails second order derivatives which leads to less accurate results. Norman et al. (1987) argue that third order schemes should be used in order to provide first-order accuracy for the Lorentz force.

In particular, in the vicinity of sudden changes in the characteristic length scale, truncation errors become very important leading to unphysical current and forces. The second order scheme makes the problem even more severe.

Powell's methods

(e.g. Powell et al. 1999, Toth 2000). B is volume centered.

Main idea is to solve the equations on conservative form but keeping the div B terms as source terms:

$$\partial_t U + \vec{\nabla} F = S$$

$$S = (0, -\vec{\nabla}\vec{B}\,\vec{B}, -\vec{\nabla}\vec{B}\,\vec{u}, -\vec{\nabla}\vec{B}\,(\vec{u}.\vec{B}))$$

Advantage: fundamental properties are preserved (e.g. Galilean invariance)

Disadvantage: equations not conservative therefore shock conditions are not satisfied.

Since B_x is not constant, the 1D problem presents now eight waves instead of seven.

A Roe-type solver is developed which propagates the eight waves.

The method works but leads sometimes to inaccurate jump relations.
See comparison in the test part (Toth 2000).

Projection methods

(e.g. Brackbill & Barnes 1980, Toth 2000, Crockett et al. 2005). B is volume centered.

Main idea: after having updated the magnetic field, calculate a correction which will ensure that div B=0.

Let us consider the Poisson equation:
The new field B' is divergenceless.

$$\Delta \phi + \vec{\nabla} . \vec{B} = 0 \rightarrow \vec{B}' = \vec{B} + \vec{\nabla} \phi$$

$$\Rightarrow \vec{\nabla} . \vec{B}' = \vec{\nabla} . (\vec{B} + \vec{\nabla} \phi) = 0$$

Note that It can be shown that for a cartesian grid this corresponds to the closest field which satisfy div B=0 (Toth 2000).

Similar method is sometimes used in incompressible hydrodynamical studies to enforce div V =0.

Advantages of the method:

-can be combined with any scheme
-B is volume centered (simple).

<u>Disadvantages of the method:</u>

-problem with energy conservation. Since B changes but not E, it implies that e is changing (can sometimes become negative).

-it is possible to recalculate the total energy to enforce conservation of internal energy, but then total energy is not conserved any more.

-the magnetic flux is not conserved. Problem may arise near discontinuities where large values of div B will be generated and where the conservation properties are essential to insure jump relations.

-a Poisson equation must be solved. Extra efforts and cpu costs. Possible problems may arise due to boundaries depending on the Poisson solver.

In practice however, the scheme seems to work well for a large set of problems and tends to be widely used (see the comparisons in the test part).
An extension has been proposed by Dedner et al. (2002) who develop hyperbolic (instead of elliptic) divergence cleaning.

Constrained transport methods

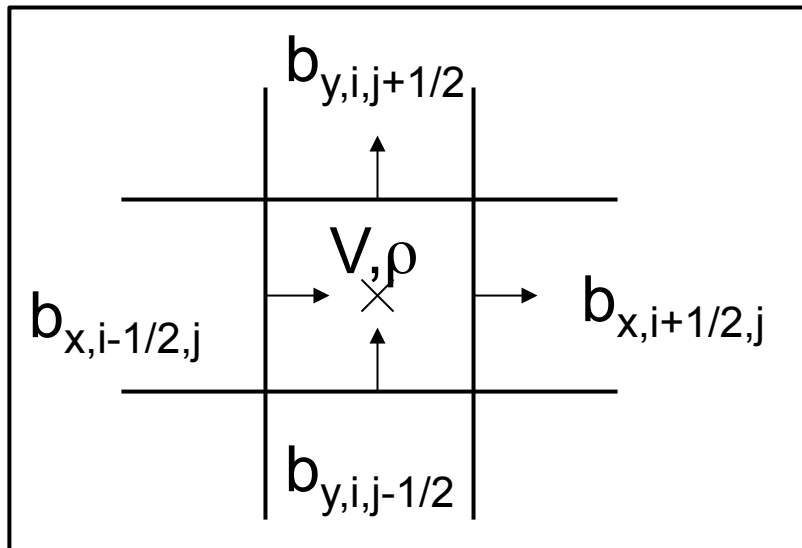(e.g. Evans & Hawley 1988, Toth 2000). B is face centered.

$$\iint \partial_t \vec{B}.d\vec{S} + \iint \vec{\nabla} \times (\vec{B} \times \vec{V})).d\vec{S} = 0$$

$$\partial_t \phi + \oint (\vec{B} \times \vec{V}).d\vec{l} = 0$$

Induction equation suggests that the relevant quantity (analogous to density) is the flux, that is the integral of the magnetic field on a surface.

It also suggests that the flux should be updated by performing some circulation on a close circuit.

Thus, magnetic field should be defined in the center of the face, the mesh is staggered.

$$\overline{b}_{x,i-1/2,j,k}(t) = \frac{1}{\Delta y \Delta z} \int_{y_{i-1/2},z_{i-1/2}}^{y_{i+1/2},z_{i+1/2}} dy' \, dz' \, b_x(t, x_{i-1/2}, y', z')$$
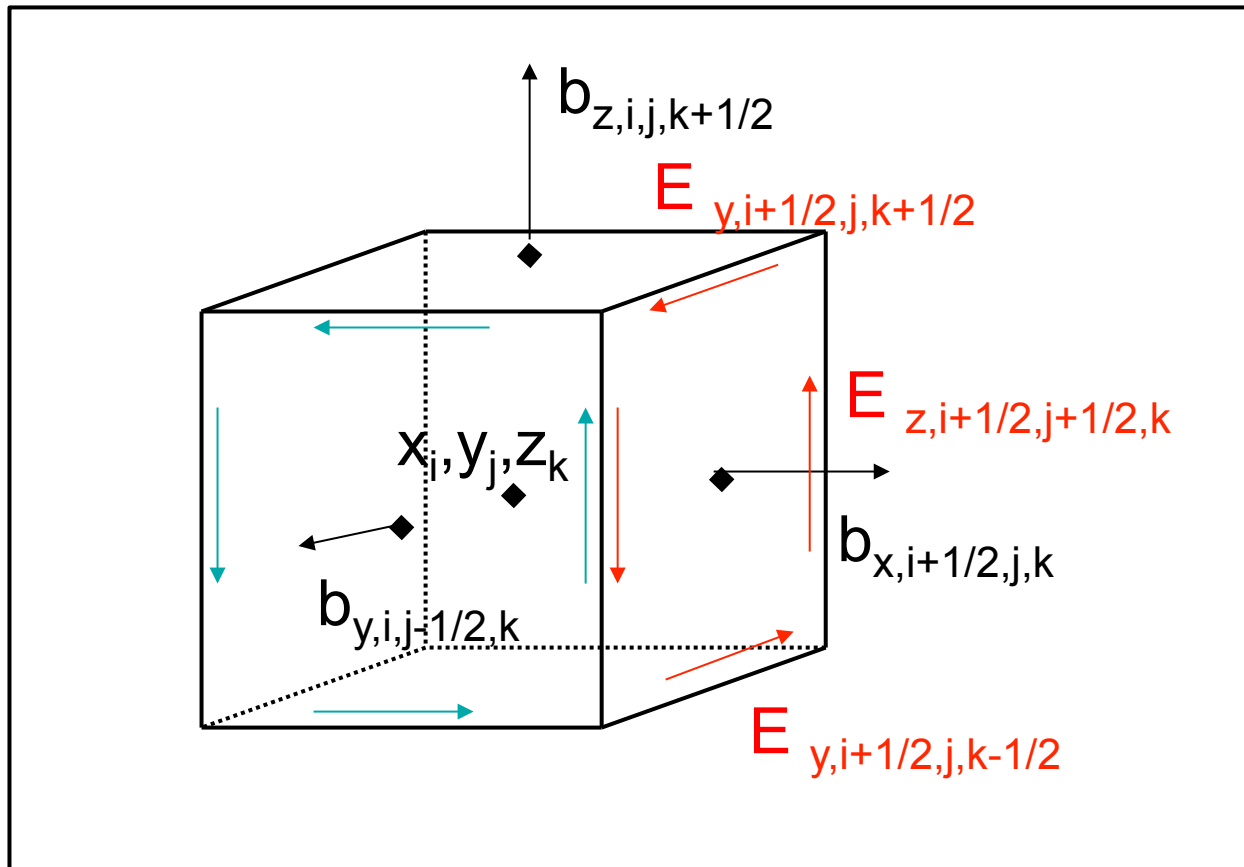
$$\overline{b}_{y,i,j-1/2,k}(t) = \frac{1}{\Delta x \Delta z} \int_{x_{i-1/2},z_{i-1/2}}^{x_{i+1/2},z_{i+1/2}} dx' \, dz' \, b_y(t, x', y_{j-1/2}, z')$$

in 3D

CT: The electric field

(e.g. Evans & Hawley 1988, Toth 2000). B is face centered.

Circulation around the faces must be performed integrating the electromotor field: VxB, located at the edges of the cells.

$b_{z,i,j,k+1/2}$

$E_{y,i+1/2,j,k+1/2}$

$E_{z,i+1/2,j+1/2,k}$

x_i, y_j, z_k

$b_{x,i+1/2,j,k}$

$b_{y,i,j-1/2,k}$

$E_{y,i+1/2,j,k-1/2}$

The equivalent of the volume averaged quantities and surface averaged flux used in Godunov type scheme is:

$$\overline{b}_{x,i-1/2,j,k}(\Delta t) = \overline{b}_{x,i-1/2,j,k}(0) + \frac{\Delta t}{\Delta y}(\overline{E}_{z,i-1/2,j+1/2,k} - \overline{E}_{z,i-1/2,j-1/2,k}) - \frac{\Delta t}{\Delta z}(\overline{E}_{y,i-1/2,j,k+1/2} - \overline{E}_{y,i-1/2,j,k-1/2})$$

$$\overline{b}_{y,i,j-1/2,k}(\Delta t) = \overline{b}_{y,i,j-1/2,k}(0) + \frac{\Delta t}{\Delta z}(\overline{E}_{x,i,j-1/2,k+1/2} - \overline{E}_{x,i,j-1/2,k-1/2}) - \frac{\Delta t}{\Delta x}(\overline{E}_{z,i+1/2,j-1/2,k} - \overline{E}_{z,i-1/2,j-1/2,k})$$

$$\overline{b}_{z,i,j,k-1/2}(\Delta t) = \overline{b}_{z,i,j,k-1/2}(0) + \frac{\Delta t}{\Delta x}(\overline{E}_{y,i+1/2,j,k-1/2} - \overline{E}_{y,i-1/2,j,k-1/2}) - \frac{\Delta t}{\Delta y}(\overline{E}_{x,i,j+1/2,k-1/2} - \overline{E}_{x,i,j-1/2,k-1/2})$$
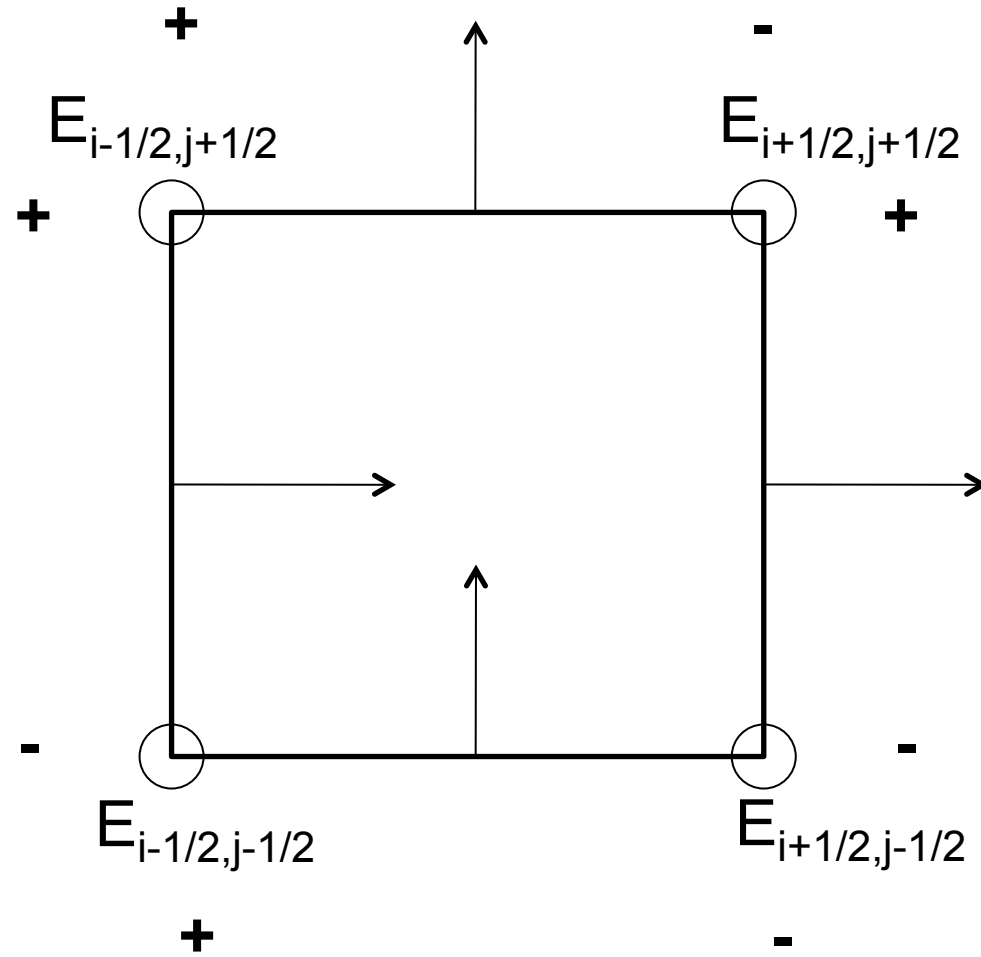
$$\overline{\overline{E}}_{x,i,j-1/2,k-1/2} = \frac{1}{\Delta t \Delta x}\int_0^{\Delta t} dt \int_{x_{i-1/2}}^{x_{i+1/2}} dx\ E_x(x, y_{j-1/2}, z_{k-1/2})$$

$$\overline{\overline{E}}_{x,i-1/2,j,k-1/2} = \frac{1}{\Delta t \Delta y}\int_0^{\Delta t} dt \int_{y_{j-1/2}}^{y_{j+1/2}} dy\ E_y(x_{i-1/2}, y, z_{k-1/2})$$

$$\overline{\overline{E}}_{z,i-1/2,j-1/2,k} = \frac{1}{\Delta t \Delta z}\int_0^{\Delta t} dt \int_{z_{k-1/2}}^{z_{k+1/2}} dz\ E_z(x_{i-1/2}, y_{j-1/2}, z)$$

As for volume averaged quantities, these expressions are exact but again approximations will be made in calculating the flux, E.

CT: Exact nullity of div B

$E_{i-1/2,j+1/2}$

$E_{i+1/2,j+1/2}$

$E_{i-1/2,j-1/2}$

$E_{i+1/2,j-1/2}$

CT: Exact nullity of div B

(e.g. Evans & Hawley 1988, Toth 2000).

With these definitions, the volume centered divergence vanishes exactly if it vanishes initially. This is shown as followed:

$$div\, b(\Delta t) =$$

$$\frac{\overline{b}_{x,i+1/2,j,k}(\Delta t) - \overline{b}_{x,i-1/2,j,k}(\Delta t)}{\Delta x} + \frac{\overline{b}_{y,i,j+1/2,k}(\Delta t) - \overline{b}_{y,i,j-1/2,k}(\Delta t)}{\Delta y} + \frac{\overline{b}_{z,i,j,k+1/2}(\Delta t) - \overline{b}_{z,i,j,k-1/2}(\Delta t)}{\Delta z}$$

$$= \frac{\overline{b}_{x,i+1/2,j,k}(0) - \overline{b}_{x,i-1/2,j,k}(0)}{\Delta x} + \frac{\overline{b}_{y,i,j+1/2,k}(0) - \overline{b}_{y,i,j-1/2,k}(0)}{\Delta y} + \frac{\overline{b}_{z,i,j,k+1/2}(0) - \overline{b}_{z,i,j,k-1/2}(0)}{\Delta z} +$$

$$\frac{\Delta t}{\Delta x \Delta y}(\overline{E}_{z,i+1/2,j+1/2,k} - \overline{E}_{z,i+1/2,j-1/2,k}) - \frac{\Delta t}{\Delta x \Delta z}(\overline{E}_{y,i+1/2,j,k+1/2} - \overline{E}_{y,i+1/2,j,k-1/2}) - (i+1/2 \leftrightarrow i-1/2)$$

$$\frac{\Delta t}{\Delta y \Delta z}(\overline{E}_{x,i,j+1/2,k+1/2} - \overline{E}_{x,i,j+1/2,k-1/2}) - \frac{\Delta t}{\Delta y \Delta x}(\overline{E}_{z,i+1/2,j+1/2,k} - \overline{E}_{z,i-1/2,j+1/2,k}) - (j+1/2 \leftrightarrow j-1/2)$$

$$\frac{\Delta t}{\Delta z \Delta x}(\overline{E}_{y,i+1/2,j,k+1/2} - \overline{E}_{y,i-1/2,j,k+1/2}) - \frac{\Delta t}{\Delta z \Delta y}(\overline{E}_{x,i,j+1/2,k+1/2} - \overline{E}_{x,i,j-1/2,k+1/2}) - (k+1/2 \leftrightarrow k-1/2)$$

$$= div\, b(0) + 0 = 0$$

Advantage of constrained transport method:

-div B vanishes to machine accuracy

-clear formulation of the average magnetic field and magnetic flux

-for some aspects, method well suited to Godunov type approaches
In particular the B_x component is already defined on the face where it is
needed to calculate the flux.

Disadvantage of the method:

-calculating the electric field is NOT straighforward (as we will see…)

-extra calculations and extra CPU costs

-for some other aspects, method not well suited to Godunov type approach
B_y component is not defined where it is needed.

Calculating the electric field: method of characteristic

(e.g. Evans & Hawley 1988, Stone & Norman 1992).

MOC: introduced by Evans & Hawley (velocity centered and B is staggered)
MOC-CT: introduced by Stone & Norman and used in ZEUS (V and B staggered).

The problem is that any electric field will ensure div B=0 as long as the CT method is used BUT stability is not ensured. Some upwinding is therefore necessary.

Evans & Hawley simply interpolate the velocity field. They use upstream interpolation (which insures stability, following approximately the characteristic) to compute the components of B.

Stone & Norman find that this method does not provide good description of the shear Alfvén waves. They take advantage of V and B being located at the same place in ZEUS and proceed as follows:

-ignoring compressibility
(discarding fast and slow waves), one can write

$$\partial_t v = \frac{B_x}{\rho} \partial_x B_y - u \partial_x v$$

$$\partial_t B_y = B_x \partial_x v - u \partial_x B_y$$

Thus:
$$\partial_t v + u \partial_x v = \frac{1}{\sqrt{\rho}} \frac{B_x}{\sqrt{\rho}} \partial_x B_y \pm \frac{1}{\sqrt{\rho}} (\partial_t B_y - B_x \partial_x v + u \partial_x B_y)$$

$$\Rightarrow \partial_t v + u \partial_x v \pm \frac{B_x}{\sqrt{\rho}} \partial_x v = \pm \frac{1}{\sqrt{\rho}} \left(\partial_t B_y + u \partial_x B_y \pm \frac{B_x}{\sqrt{\rho}} \partial_x B_y \right)$$

$$\Rightarrow \partial_t \left(v \mp \frac{B_y}{\sqrt{\rho}} \right) + (u \pm v_a) \partial_x \left(v \mp \frac{B_y}{\sqrt{\rho}} \right) = 0$$

This implies that $v +/- B_y/\rho^{1/2}$ follows the characteristics with velocity $u +/- B_x/\rho^{1/2}$ and are therefore invariant along them.

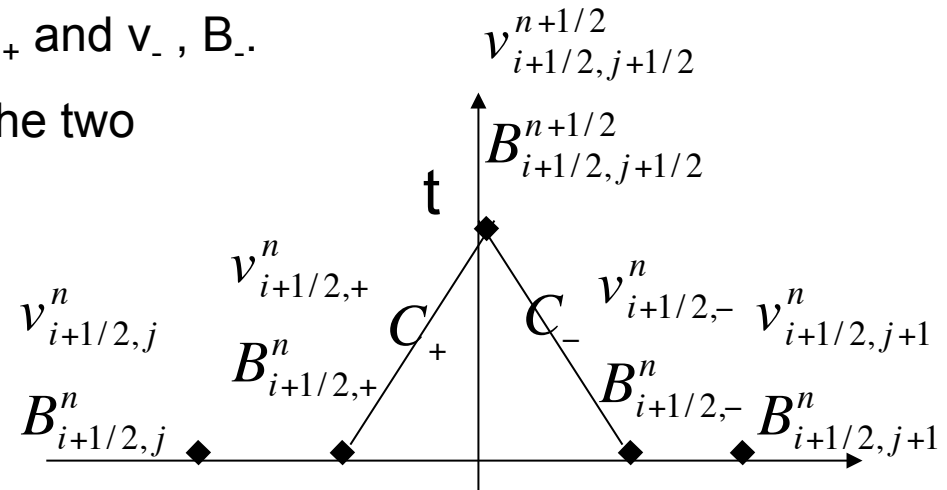$$(v_{i+1/2,j+1/2}^{n+1/2} - v_{i+1/2,+}^{n}) - (B_{y,i+1/2,j+1/2}^{n+1/2} - B_{y,i+1/2,+}^{n})/\sqrt{\rho_+} = 0$$

$$(v_{i+1/2,j+1/2}^{n+1/2} - v_{i+1/2,-}^{n}) - (B_{y,i+1/2,j+1/2}^{n+1/2} - B_{y,i+1/2,-}^{n})/\sqrt{\rho_-} = 0$$

Thus one needs to determine v_+, B_+ and v_-, B_-.

This is achieved by tracking back the two

characteristics as shown in the

graph:

Calculating the electric field: field interpolation
(Dai & Woodward 1998, Toth 2000).

Idea: estimate the electric field by interpolating the velocity and magnetic field variables

Dai & Woodward interpolate the variables and proceed as follows:
-at time t, the staggered field $b_{x,i+1/2,j}$, $b_{y,i,j+1/2}$, is known.
-simple average gives the centered magnetic field: $B_{x,i,j} = 1/2(b_{x,i-1/2,j} + b_{x,i+1/2,j})$.
-solve the 4 (6 in 3D) Riemann problems leading to new centered magnetic field B
-obtain estimated edge centered magnetic and velocity field through:

$$\vec{B}_{i+1/2,j+1/2}^{n+1} = \frac{1}{4}\left(\vec{B}_{i,j}^{n+1} + \vec{B}_{i+1,j}^{n+1} + \vec{B}_{i,j+1}^{n+1} + \vec{B}_{i+1,j+1}^{n+1}\right), \vec{u}_{i+1/2,j+1/2}^{n+1} = \frac{1}{4}\left(\vec{u}_{i,j}^{n+1} + \vec{u}_{i+1,j}^{n+1} + \vec{u}_{i,j+1}^{n+1} + \vec{u}_{i+1,j+1}^{n+1}\right)$$

$$\vec{B}_{i+1/2,j+1/2}^{*} = \frac{1}{2}\left(\vec{B}_{i+1/2,j+1/2}^{n+1} + \vec{B}_{i+1/2,j+1/2}^{n}\right), \vec{u}_{i+1/2,j+1/2}^{*} = \frac{1}{2}\left(\vec{u}_{i+1/2,j+1/2}^{n+1} + \vec{u}_{i+1/2,j+1/2}^{n}\right)$$

$$\overline{E}_{i+1/2,j+1/2} = E\left(\vec{B}_{i+1/2,j+1/2}^{*}, \vec{u}_{i+1/2,j+1/2}^{*}\right)$$

-finally compute new b (face centered magnetic field) by CT method.

Preserve div B=0 but no upwinding => likely unstable

Calculating the electric field: flux interpolation

(Ryu et al. 1999, Balsara & Spicer 1999, Toth 2000, Ziegler 2005).

Idea: estimate the electric field by interpolating the fluxes computed at the face center

Balsara & Spicer interpolate proceed as follows:
-at time t, the staggered field $b_{x,i+1/2,j}$, $b_{y,i,j+1/2}$, is known
-solve the 4 Riemann problems gives 4 fluxes at the face center
-obtain the electric field at the edge (along z) by simple flux averaging

$$with \ \partial_t U + \partial_x F + \partial_y G = 0,$$

$$F_7 = -E_z, \quad G_6 = E_z,$$

$$E^{n+1/2}_{i+1/2,j+1/2} = \frac{1}{4}\left(G^{n+1/2}_{6,i+1/2,j} + G^{n+1/2}_{6,i-1/2,j} - F^{n+1/2}_{7,i,j+1/2} - F^{n+1/2}_{7,i,j-1/2} \right)$$

-finally compute new b (face centered magnetic field) by CT method.

However, with this formulation the flux of a 1D problem calculated with a 2D code is not identical to the flux obtained with a 1D code. Ryu et al. (1999) present a slightly different formulation which has this property.

Preserve div B=0 but no « proper » upwinding => likely unstable
(some upwinding in flux calculations)

Calculating the electric field: 2D Riemann solver

(Londrillo & Del Zana 2000, 04, Gardiner & Stone 2005, Fromang et al. 2006).

Most recently, it has been realized that electric field should be upwinded in a similar way than in the cell centered formulation. Formally, the problem can be thought as a 2D Riemann problem. That is 4 states are now interacting instead of 2. Proper flux estimate can be performed following this line, ensuring stability.

Londrillo & Del Zana and Fromang et al. proceed as follow:
-consider a linear solver (like Roe solver)
-in the 1D case, the flux is:

-a natural 2D generalisation of this is:

U_{LR}	$U_{R\,R}$
U_{LL}	U_{RL}

$$F(U(0)) = \frac{1}{2}(F_L + F_R) + \frac{1}{2}\sum_{i=1,m}\left|\tilde{\lambda}_i\right|(\tilde{\beta}_i - \tilde{\alpha}_i)\tilde{K}^i$$

$$F(U(0)) = \frac{1}{4}(F_{LL} + F_{RL} + F_{LR} + F_{RR}) +$$

$$\frac{1}{2}\sum_{i=1,m}\left|\tilde{\tilde{\lambda}}_{x,i}\right|(\tilde{\tilde{\beta}}_{x,i} - \tilde{\alpha}_{x,i})\tilde{K}^i_x - \frac{1}{2}\sum_{i=1,m}\left|\tilde{\tilde{\lambda}}_{y,i}\right|(\tilde{\tilde{\beta}}_{y,i} - \tilde{\alpha}_{y,i})\tilde{K}^i_y$$

where the 2 Roe matrix are constructred by considering:

$$\tilde{\tilde{\lambda}}^i_x, \tilde{K}^i_x \rightarrow \overline{U}_{x,L} = \frac{1}{2}(U_{LL} + U_{LR}), \overline{U}_{x,R} = \frac{1}{2}(U_{RL} + U_{RR})$$

$$\tilde{\tilde{\lambda}}^i_y, \tilde{K}^i_y \rightarrow \overline{U}_{y,L} = \frac{1}{2}(U_{LL} + U_{RL}), \overline{U}_{y,R} = \frac{1}{2}(U_{LR} + U_{RR})$$

Calculating the electric field: 2D Riemann solver

(Londrillo & Del Zana 2004).

For non linear solver, like HLL, there is no systematic way of generalising the solver and this can be tricky.

For HLL, a natural generalisation can be obtained (Londrillo & Del Zana, 2004). It takes advantage of the staggered mesh and assume that the problem entails only 4 waves by taking e.g. $\lambda_{x,R}=\max(\lambda_{x,RL},\lambda_{x,RR})$.
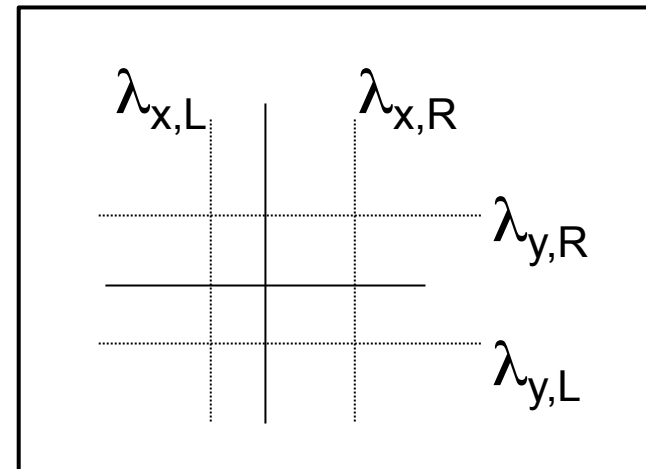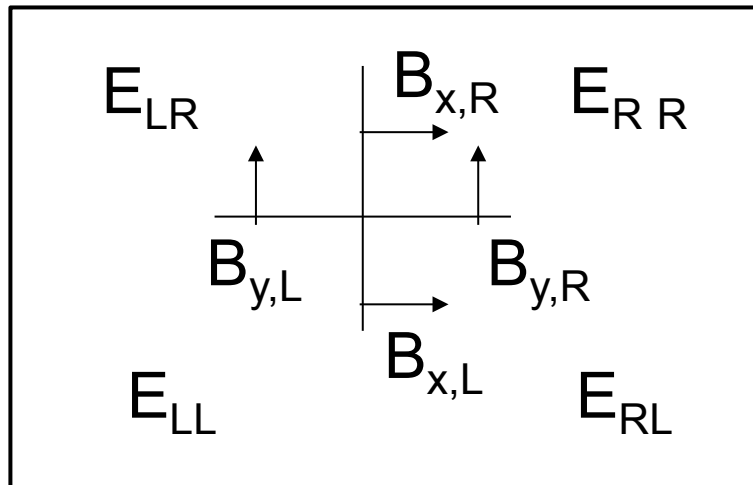
$$E^* = \frac{\lambda_{x,R}\lambda_{y,R}E_{LL} + \lambda_{x,L}\lambda_{y,L}E_{RR} - \lambda_{y,R}\lambda_{x,L}E_{RL} - \lambda_{y,L}\lambda_{x,R}E_{LR}}{(\lambda_{x,R} - \lambda_{x,L})(\lambda_{y,R} - \lambda_{y,L})}$$

$$-\frac{\lambda_{y,L}\lambda_{y,R}}{\lambda_{y,R} - \lambda_{y,L}}(B_{x,R} - B_{x,L}) + \frac{\lambda_{x,L}\lambda_{x,R}}{\lambda_{x,R} - \lambda_{x,L}}(B_{y,R} - B_{y,L})$$
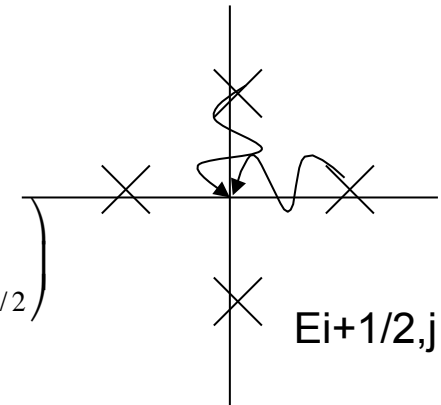
Calculating the electric field: 2D Riemann solver
(Gardiner & Stone 2005).

Gardiner & Stone present another approach slightly different but not far from the 2D solver methodology.

They transport the electric field calculated at the 4 neighbouring face center (given by the 4 1D Riemann problems), writing:

$$E_{z,i+1/2,j+1/2} = \frac{1}{4}\left(E_{z,i+1/2,j} + E_{z,i-1/2,j} + E_{z,i,j+1/2} + E_{z,i,j-1/2}\right)$$

$$+ \frac{dy}{8}\left(\frac{\partial E_z}{\partial y}\bigg|_{i+1/2,j+1/4} - \frac{\partial E_z}{\partial y}\bigg|_{i+1/2,j+3/4}\right) + \frac{dx}{8}\left(\frac{\partial E_z}{\partial x}\bigg|_{i+1/4,j+1/2} - \frac{\partial E_z}{\partial x}\bigg|_{i+3/4,j+1/2}\right)$$

Ei+1/2,j

Then the « gradient » of the electric field are estimated with induction equation and some upwind procedure (e.g. Lax-Friedrich solver).

Calculating the electric field: 2D Riemann solver

In all the former cases, the 1D flux is exactly recovered in the limit when the 2D flow becomes equivalent to a 1D situation.

The solvers are all properly upwinded therefore ensuring numerical stability.

Numerical tests indicate that this approach is indeed robust and accurate.

One disadvantage is its cost since 4 (8) bidimensional Riemann solvers have to be solved for each cell in 2D (3D).

In the same way, reconstruction must also be performed at the edge and not only in the face center.

Reconstruction of V and B for 2nd order accuracy of the Lorentz force

b_x is already in place !
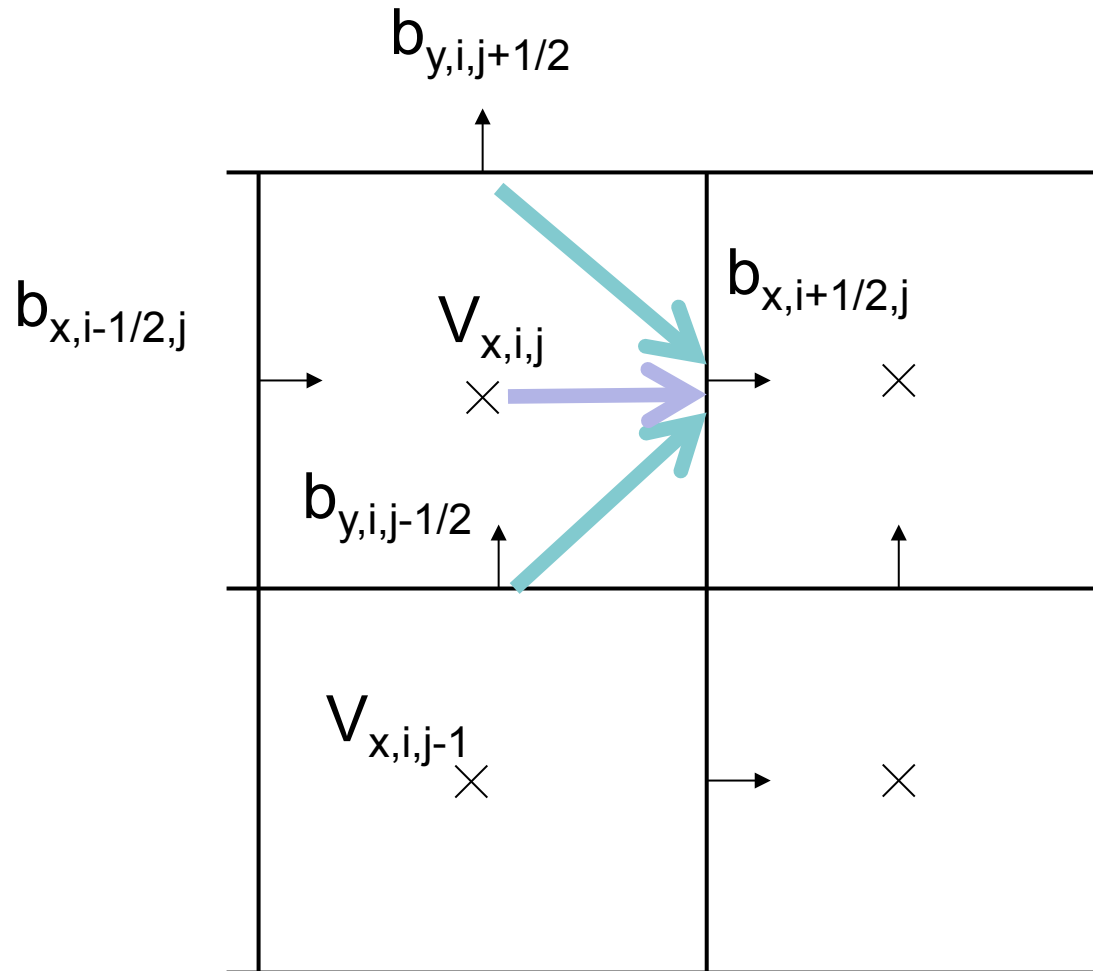
Reconstruction of V and B for 2nd order accuracy of the electric field at the edge
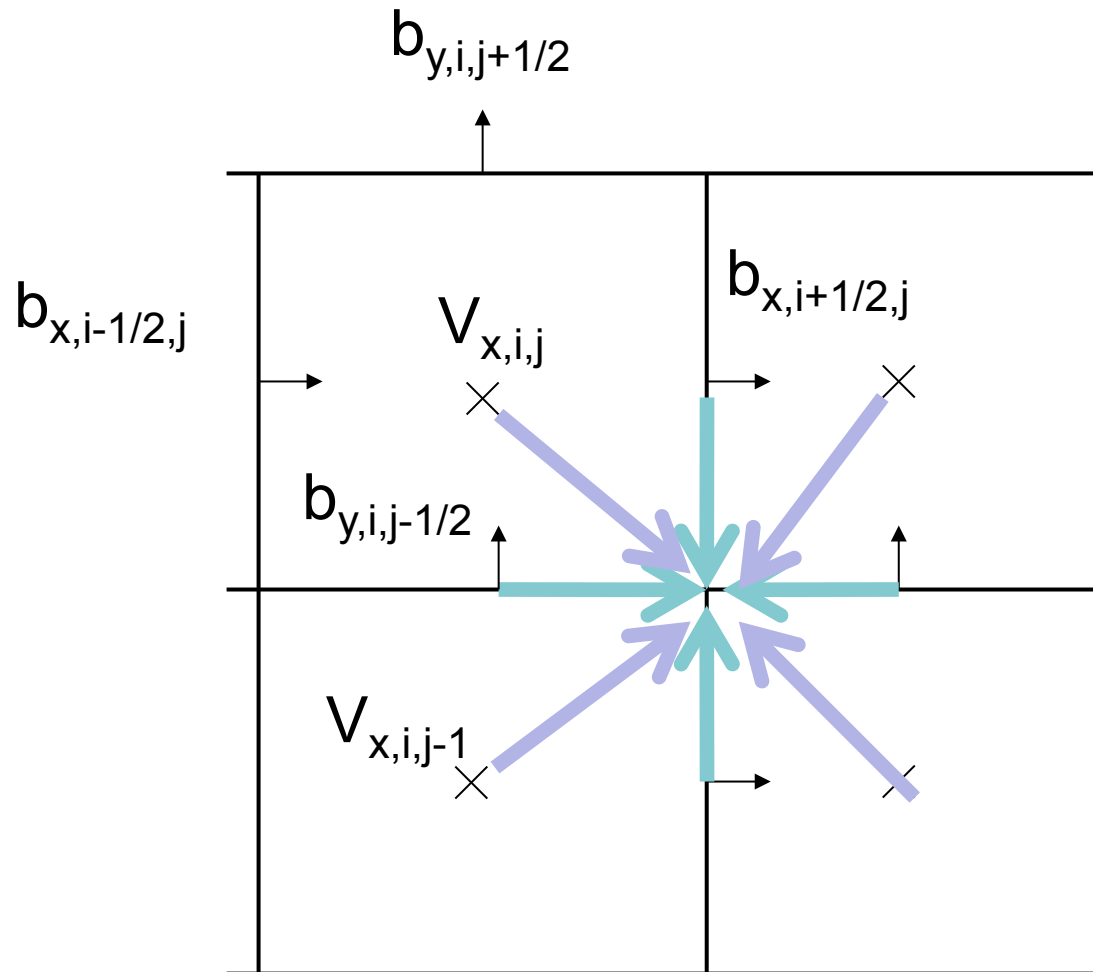
2D tests: testing the method

Rotated shock tube test (Toth 2000), look at B_{para} which ideally
Is constant.

8-waves: incorrect jump
and large errors

Projection: large errors
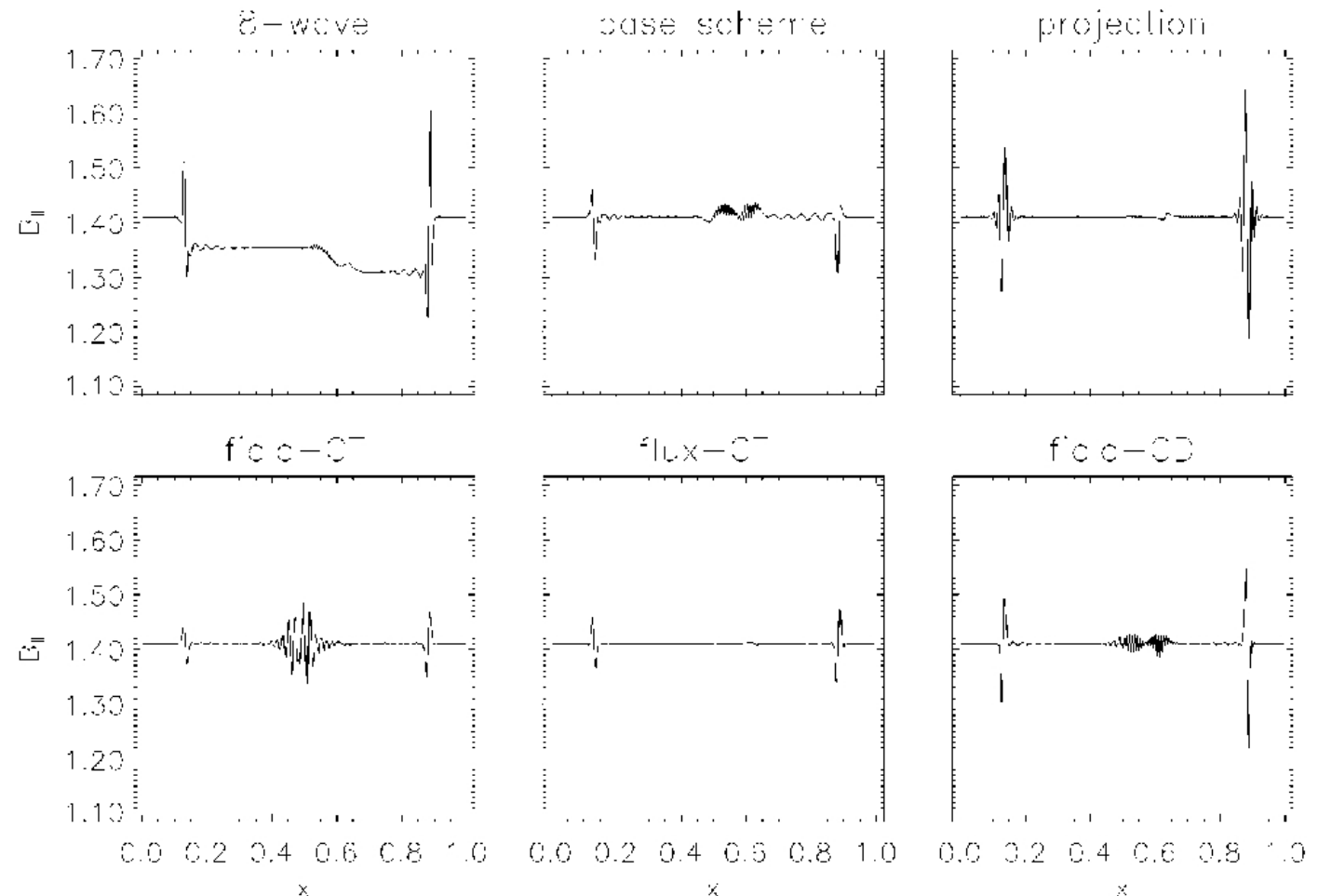
CT methods: smaller
errors

Flux-CT is the best

FIG. 11. The parallel component of the magnetic field in the 2D rotated shock tube test is shown for six different schemes. The analytic solution is a uniform value $B_{\parallel} = 5/\sqrt{4\pi}$. The non-conservative 8-wave formulation is in error by several percentage everywhere between the left and right moving fast shocks ($x = 0.1 - 0.9$). The conservative schemes, including the base-scheme (middle top panel), show significant errors close to the discontinuities only.

2D tests: testing the method

Orszag-Tang Vortex

Toth 2000

8-wave

Flux interpolation
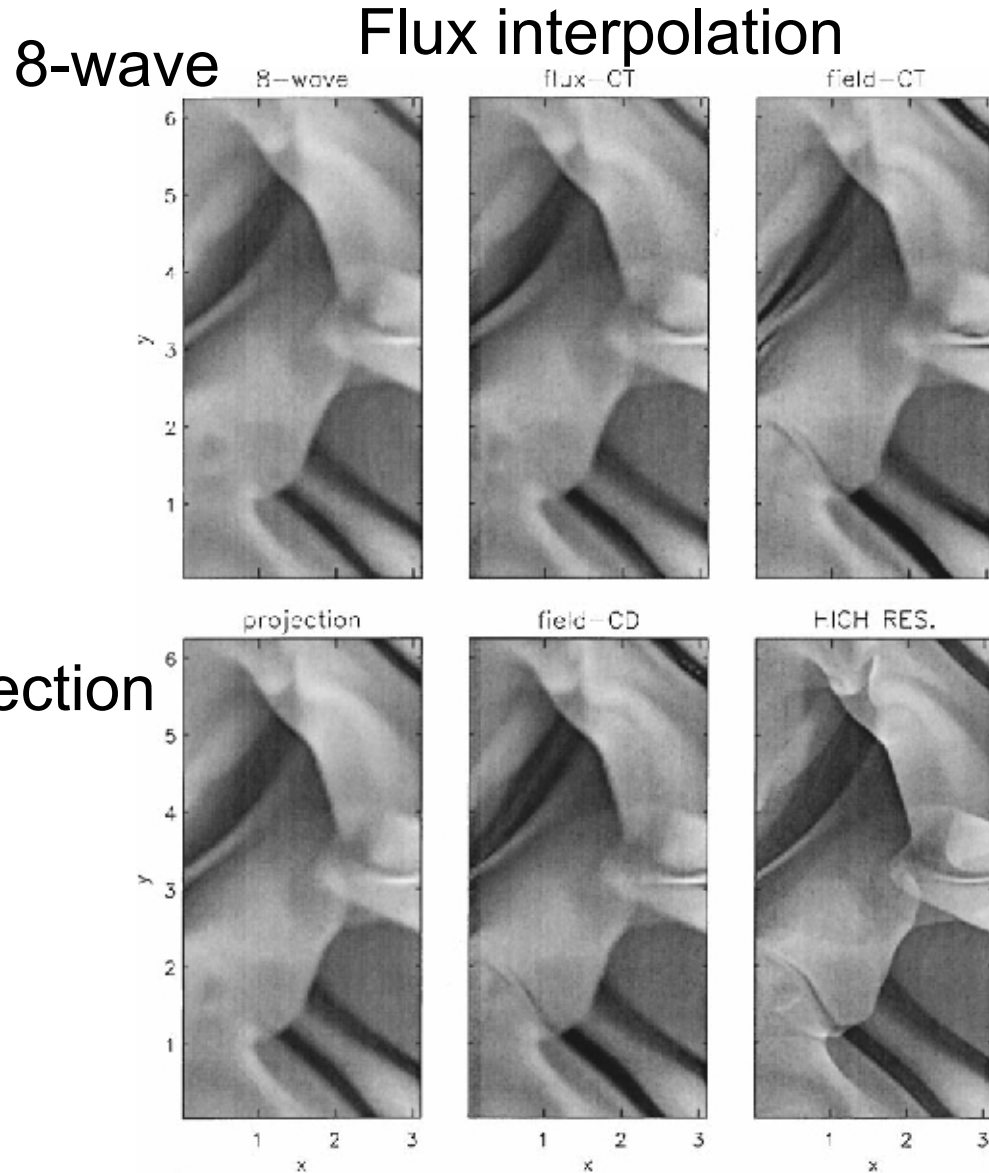
Field interpolation

projection

High resolution

FIG. 16. The temperature distribution in the Orszag–Tang vortex problem. Only the left half of the computational domain is shown, the other half is symmetric. The five schemes are compared at a 100 × 100 resolution. The reference high resolution solution (bottom right panel) was computed on a 400 × 400 grid with the projection
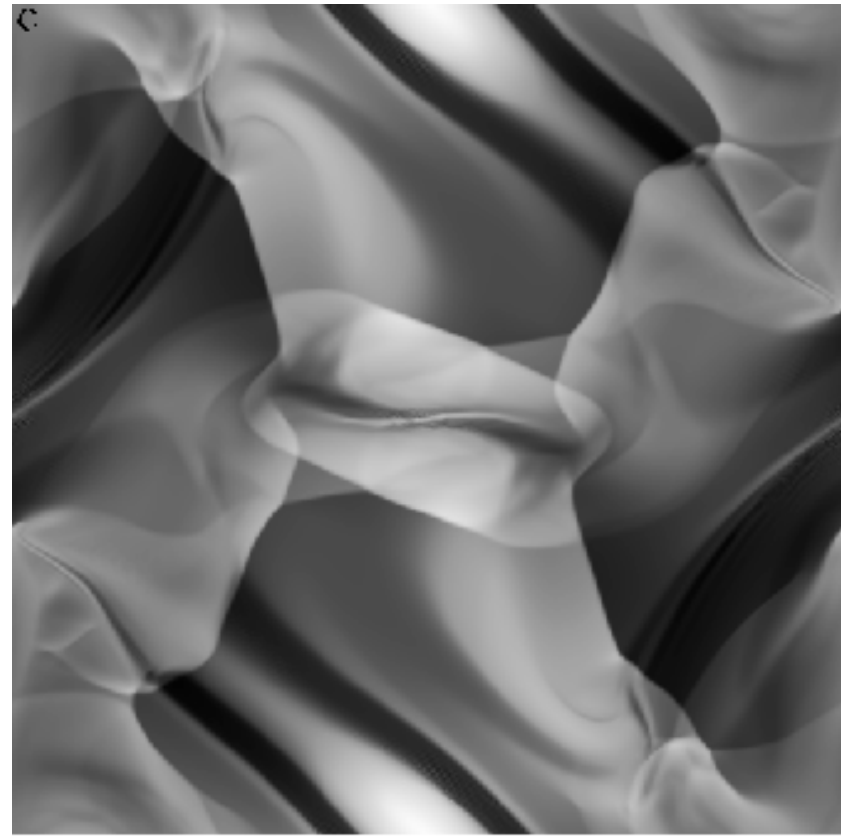
2D tests: code comparison

Orszag-Tang vortex resolution 512
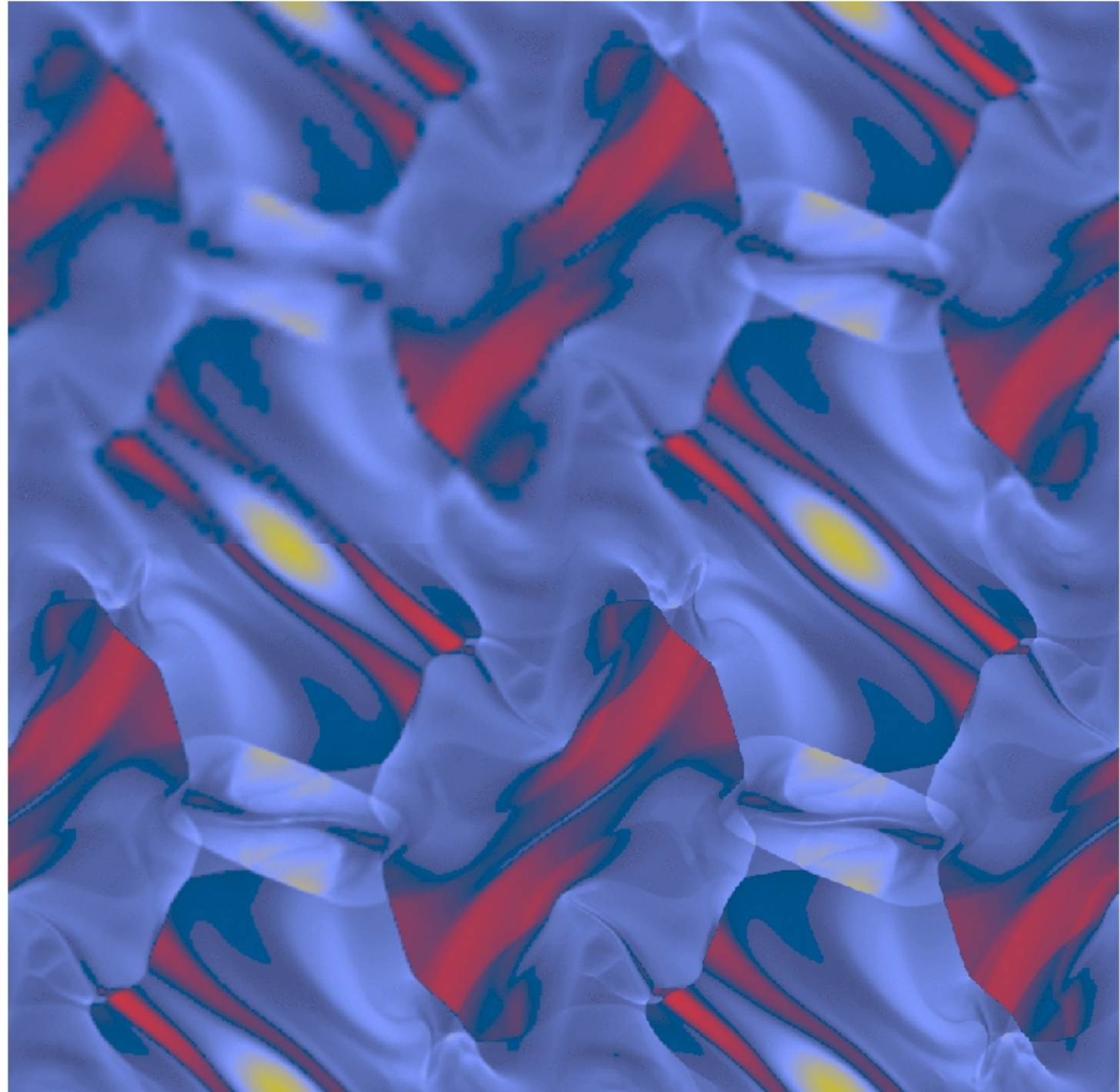
Fromang et al. 2006 (Ramses)
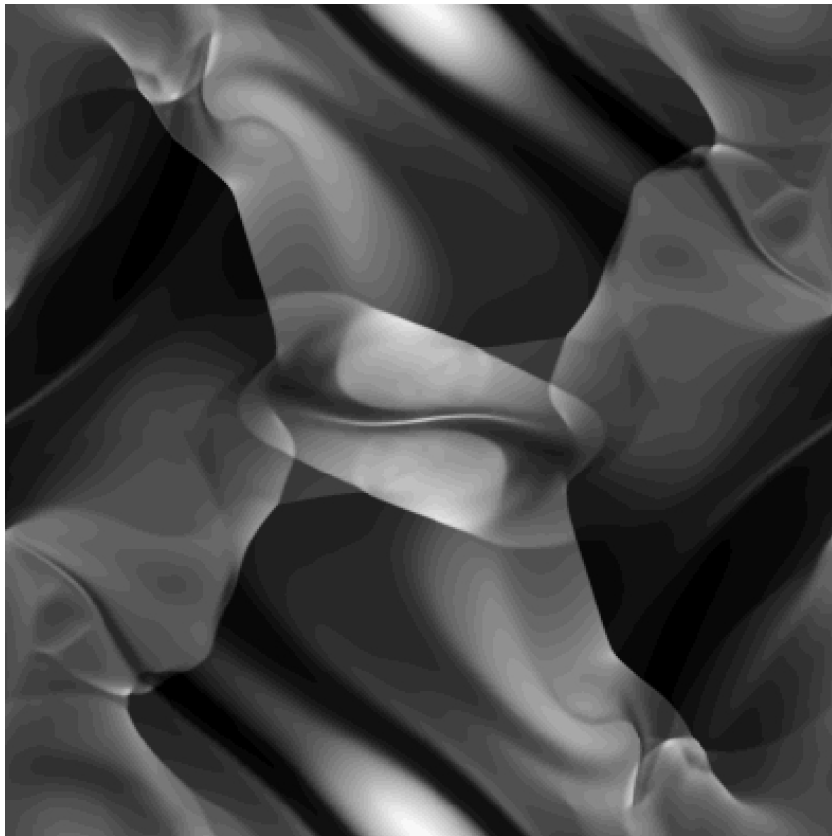
Dai & Woodwards 1998

Athena code

Ortzag-Tang Vortex

4 resolutions
64,128,256,
512

2D tests: testing the method

Fast rotor (Toth 2000):

Taken from Mouschovias & Paleologou 1980, first done by Balsara & Spicer 1999

A dense cylinder rotates inside a diffuse medium, a transverse magnetic field threaded the 2-media.
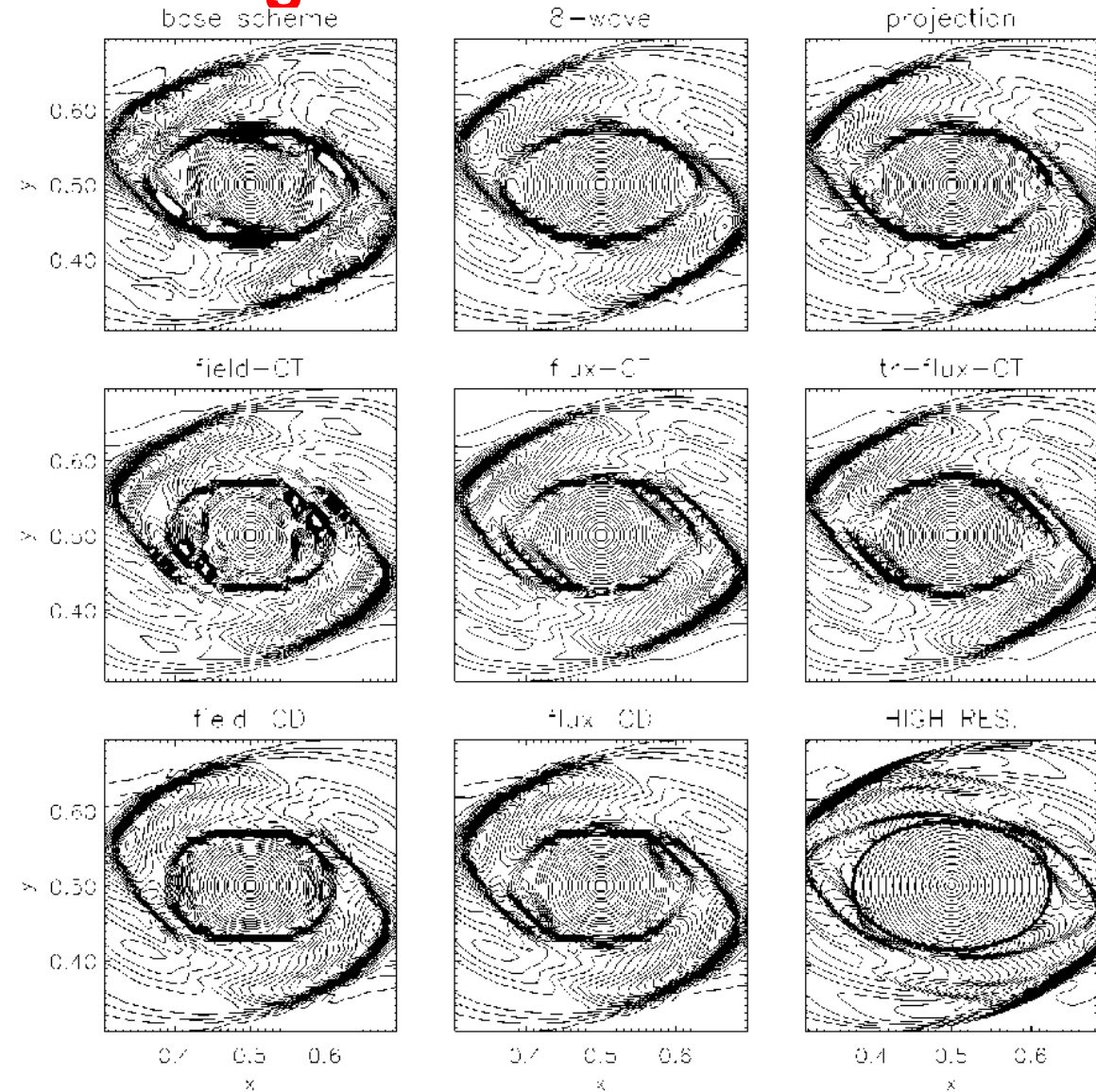

FIG. 20. The Mach number $|v|/c_s$ for the second rotor problem in the central part of the computational dom The seven schemes and the base scheme are compared at a 100×100 resolution. The reference high resolu solution (bottom right panel) was computed on a 400×400 grid with the projection scheme. The 30 contourl are shown for the Mach number ranging from 0 to 3.3.

References:

Balsara, D., 2001, JCP 174, 614

Balsara, D., Spicer, D., 1999, JCP, 153, 671

Brackbill, J., Barnes, D., 1980, JCP, 35, 426

Brio, M., Wu, C., 1988, JCP, 75, 400

Cargo, P., Gallice, G., 1997, JCP, 136, 446

Crockett, R., Collela, P., Fisher, R., Klein, R., McKee, C., JCP, 203, 422

Dai, W., Woodwards, P., 1998, 494, 317

Davis, S., 1988, SIAM, J., Sci. Stati., 9, 445

Dedner, A., Kemm, F., Kroner, D., et al. 2002, JCP, 175, 645

Dorfi, E., JCP, 43, 1

Einfeld, B., Munz, C., Roe, P., Sjogreen, B., 1991, JCP, 92, 273

Evans, C., Hawley, J., 1988, ApJ, 33, 659

Fromang, S., Hennebelle, P., Teyssier, R., 2006, A&A, 457, 371

Gardiner, T., Stone, J., 2005, JCP, 205, 509

Godunov, A., 1959, Mat. Sb., 47, 357

Gurski, K, 2004, SIAM J., SCI Comput, 25, 2165

Harten, A., Lax, P., Van Leer, B., 1983, SIAM review, 25, 35

Londrillo, P., Del Zanna, L., 2000, ApJ, 530, 508

Londrillo, P., Del Zanna, L., 2000, JCP, 195, 17

Linde, T., 2002, Int. J. Numer. Methods Fluids 40, 391

Miyoshi, T., Kusano, K, 2005, JCP, 208, 315

Powell, K., Roe, P., Linde T. et al., 1999, JCP, 154, 284

Roe, P., 1981, JCP, 53, 357

Ryu, D., Miniati, F., Jones, T., Franck, A., 1998, ApJ, 509, 244

Stone, J., Norman, M., 1992, ApJS, 80, 791

Toth, G., 2000, JCP, 161, 605

Toro 1999, Riemann Solvers and Numerical Methods for fluid dynamics, Springer

Ziegler, U., A&A, 435, 385